Article:
Brinza, L, Geraki, K, Matamoros Veloza, A orcid.org/0000-0002-3870-9141 et al. (2 more authors) (2021) The Irish kelp, Fucus vesiculosus, a highly potential green bio sorbent for Cd (II) removal: Mechanism, quantitative and qualitative approaches. Journal of Cleaner Production, 327. 129422. ISSN 0959-6526

https://doi.org/10.1016/j.jclepro.2021.129422

The Irish kelp, *Fucus vesiculosus,* a highly potential green bio sorbent for Cd (II) removal: mechanism, quantitative and qualitative approaches

Loredana Brinza[a*], Kalotina Geraki[b], Adriana Matamoros-Veloza[c], Maria Ignat [d], Mariana Neamtu[a]

[a] "Alexandru Ioan Cuza" University of Iasi, Institute of Interdisciplinary Research, Department of Exact Sciences and Natural Sciences, Iasi, 700107, Romania

[b] Diamond Light Source, Harwell Science and Innovation Campus, Didcot, OX11 0DE, Oxfordshire, United Kingdom

[c] University of Leeds, School of Mechanical Engineering, Leeds, LS2 9JT, Yorkshire, United Kingdom

[d] "Alexandru Ioan Cuza" University of Iasi, Faculty of Chemistry, Iasi, 700107, Romania

Abstract

Looking for new green and environmentally friendly bio sorbents for metal removal from polluted wastewater, the present study investigates the potential new bio sorbent for Cd(II) removal from wastewater namely, the mechanism and uptake capacity of Cd(II) by brown algae, *Fucus vesiculosus* from the Irish Sea. This work takes a comprehensive approach involving the combination of qualitative and quantitative information collected from macro to atomistic scale, in a direct and non-destructive manner. Our results demonstrate that Cd(II) is adsorbed on the algal surface based on carboxylic of alginate groups. Effective Cd(II) adsorption is achieved at pH conditions between 5 and 7, at which the uptake occurs rapidly (~2 h), with increasing Cd(II) concentration. Cd maximum uptake capacity (i.e., 1.203 mmol Cd g^{-1} dried algae) in first adsorption cycle show superior uptake as opposed to other species. Quantitatively the bio sorbent has an increasing uptake capacity (more than two folds) in the second cycle, after metal elution and biomass surface sites functioning. Desorption of Cd(II) and the regeneration of the biomass is effectively achieved with HCl (10 mM) and EDTA (1mM), but they can only be used for two cycles, before the efficiency decreases. Microprecipitation occurs at high pH (>9) when using NaOH as an eluent. Results from this work shed new light on understanding Cd(II) binding mechanisms on *Fucus v.*, providing crucial information for further process optimization, pilot testing,

* Corresponding author: Tel.: + 40-232-201102. E-mail address: loredana.brinza@uaic.ro

scaling up and implementation as a clean, environmentally friendly biotechnology applied to wastewater treatments.

Keywords: Cadmium ion, Irish *Fucus vesiculosus*, adsorption, synchrotron spectroscopy, quantitative and qualitative uptake, algae reuse.

Introduction

Laboratory studies have shown the promising use of green and environmentally friendly biotechnologies for removal of toxic species from wastewater and soils (Ahmed et al., 2017; Brinza et al., 2005, 2007; Gavrilescu and Chisti, 2005; Hayat et al., 2017; Işıldar et al., 2019; Kapahi and Sachdeva, 2019; Rodriguez-Couto et al., 2021; Saxena et al., 2020; Schlosser, 2020; Shah et al., 2021). They used different algal species to uptake, remove, immobilize, totally or partially degrade toxic species through biosorption, bioaccumulation, bioconversion, biodegradation and bio catalysis (Ahmed et al., 2017; Schlosser, 2020). These methods use green products (i.e., whole or parts of raw biomass), waste bioproducts from other industrial processes or marine abundant species that may pose a threat in specific settings (e.g., algae bloom on naval traffic) (Gavrilescu, 2004; Mazur et al., 2018). Biosorption is one of the methods commonly used because of its high uptake efficiency, selectivity, biomass reusability and low cost(Abbas et al., 2014; Arumugam et al., 2018; Brinza et al., 2007; Bwapwa et al., 2017; Davis et al., 2003; He and Chen, 2014; Kanchana et al., 2014; Sweetly, 2014; Zeraatkar et al., 2016). One interesting approach is the reuse of biomass material in subsequent cycles by the elution of already adsorbed metals. When exhausted after a final elution for decontamination the bio sorbent may be safely disposed; closing the life cycle of both components involved in the bio sorption process and making the application sustainable (Gavrilescu and Chisti, 2005; Mazur et al., 2018; Sweetly, 2014; Zeraatkar et al., 2016). Practices such us making usage of waste industrial product, product recycling, reuse, and final disposal of biomass as fertilizer, ensure the requirements of a green, circular and eco-friendly clean up technology as well as the 6Rs concepts that are in the support of sustainable products and development and life sustainability (Bdour et al., 2009; D'Amato et al., 2017; Raftowicz-Filipkiewicz, 2016; Santibanez Gonzalez et al., 2019; Werkneh and Rene, 2019).

Several studies have shown that brown algae species have better adsorption capabilities that their counterparts, green and red species, likely because of their high polysaccharide content within their tissue and cell walls which are mostly responsible for meal binding (Davis et al., 2003; Fernandez et al., 2018; Hannachi and Hafidh, 2020; He and Chen, 2014; Kanchana et al., 2014; Kizilkaya et al., 2012a; Kizilkaya et al., 2012b; Mata et al., 2009; Mazur et al., 2017; Zeraatkar et al., 2016). Macromolecular quantitative studies, that were manly obtained from laboratory studies using monion synthetic solutions, have demonstrated that brown algae can uptake Cd(II) behaving simultaneously as a cationic ion-exchange resin and as a bio sorbent. Particularly, our previous research has been focused on brown Irish kelp, that has not been study before as a potential bio sorbent for metals. First quantitative and qualitative investigations that considered Zn uptake from Zn polluted waters, showed promising uptake capacity for Zn (ca 0.5 mmol g^{-1}) and initial comparative studies indicated even higher potential for Cd.,. However, the complex uptake process depends on process conditions and metal chemistry in solution as well as bio-sorbent related parameters (i. e., algae habitat, metabolism, seasonal growth) (Brinza et al., 2007; Brinza et al., 2009; Cardoso et al., 2017; Cardoso et al., 2016; He and Chen, 2014; Kizilkaya et al., 2012b; Luna et al., 2010; Mata et al., 2009; Mazur et al., 2018; Mazur et al., 2017; Romera et al., 2007), thus it mechanisms as well as maximum uptake capacity needs to be clearly identified for each individual metal - sorbent system at laboratory scale before testing the bio sorbent on real effluents and scaling up to pilot or industrial level.

Understanding the mechanism of metals uptake is very significant aspect of the biosorption process, as brings crucial molecular information that will help in: further bio sorbent manipulation/ pre-treatment, making the choice of an efficient eluent for metal recovery and bio sorbent reuse in repetitive adsorption-desorption cycles. Various approaches have used to evaluate the uptake mechanism and quantify adsorption of metals on bio sorbents. For example, estimation of adsorption using kinetic models that compare different adsorbents at similar conditions (process and environmental) through specific parameters (e.g., weighed uptake capacities, adsorption rates and contact time to reach equilibrium) (He and Chen, 2014; Mata et al., 2008; Mazur et al., 2018; Moreira et al., 2019; Nasab et al., 2017; Sari and Tuzen, 2008). Kinetic models use various assumptions that do not represent real conditions and, therefore, they only provide limited indirect and empiric information (Fang et al., 2020; Ho, 2006; Hubbe et al., 2019; Nie et al., 2016; Simonin, 2016; Wu et al., 2009; Yuh-Shan, 2004). Fourier Transform Infrared (FTIR) spectroscopy has been also used to derive mechanistic information on metals

sorption under various process conditions, providing information about organic molecules (e.g., carboxyl, ether, alcoholic, and amino groups) that are potentially involved in metals binding (Ahmady-Asbchin and Jafari, 2013; Fang et al., 2011; Herrero et al., 2006; Jayakumar et al., 2015; Kaparapu and Prasad, 2018; Moreira et al., 2019; Sheng et al., 2004). High resolution in-situ synchrotron techniques such as X-ray Absorption Spectroscopy (XAS) and X-ray Fluorescence (XRF) allow direct measurement of unaltered metal bonding environment at atomic scale and its micro spatial distribution (Brinza et al., 2014; Diaz-Moreno et al., 2012), this help us to unveil mechanistic information at molecular level and to understand the adsorption process in greater detail. Few studies have used synchrotron techniques to study metal binding mechanisms on various bio matrices (e.g., mussels, mosses, leaves, algae) which have demonstrated that these techniques provide direct speciation information without metal specie alteration(González et al., 2016; Huguet et al., 2012; Manceau et al., 2019; Mari et al., 2015; Yan et al., 2020). Our previous laboratory based, supplemented by synchrotron investigations on zinc [Zn(II)] adsorption onto marine kelp *Fucus vesiculosus* (Brinza et al., 2019; Brinza et al., 2020) allowed us to elucidate combined mechanisms for Zn(II) sorption on the complex and heterogeneous algae surface (ion exchange of light metals, H bonding, covalent bonding with carboxyl functional groups from alginate and cellulose components of the algae cell wall, in specific proportions as a function of pH, metal concentration and algae dosage or metal/sorbent/solution ratios). Qualitatively, the synchrotron micro X Ray analyses showed direct evidence of Zn bonding by carboxylic functional groups preponderantly of alginate and less cellulose components of the algae cell wall, Zn been surrounded by 5 - 6 oxygens at atomic distance of 1.98-2.03 Å(Brinza et al., 2019).

Comparative quantitatively, the results suggested that particularly the Irish *Fucus v.* as opposed to other algae or *Fucus v.* from other seas, is a promising material to become bio sorbent for Zn and other cations with high toxicity (e.g., Cd(II), Cr(VI), Pb(II), etc). Accounting on the potential seen in our previous results (i.e., for Zn), the need of investigating the maximum uptake capacity and the mechanism of the Irish kelp for other metals has raised. Although generally from metals chemistry point of view metals may behave similarly in solution, their chemical speciation differs slightly as a consequence of their variation in electronegativity. Thus, their adsorption on sorbents varies significantly, fact that was seen comparatively in our previous study at a low and single metal concentration: Cd(II) was adsorbed almost twice as Zn on the dried Irish kelp (Brinza et al., 2019). In this work, we extend our previous investigations of metals biosorption onto dried algal biomass *Fucus vesiculosus* from the Irish Sea, in

particular, focusing on quantitative and qualitative assessments of cadmium [Cd(II)] uptake using the novel synchrotron approach besides the ordinary laboratory based and modelling ones.

Our goal is to study Cd(II) sorption capacity and mechanism onto *Fucus v.* as a cleaner alternative for Cd(II) removal, which is compatible with current water treatments, addressing the following research questions as objectives: (i) what are the optimum pH value(s) at which maximum Cd(II) adsorption is reached? (ii) Cd (II) adsorption on *Fucus v.* is reversible? So, we can use the bio substrate in repetitive cycles? (iii) which eluent will reach highest elution efficiency? (iv) can we regenerate the absorption capacity of the biomass after elution to ensure sustainable use? (v) what are the species involved in the adsorption process and the mechanisms involved?

Materials and Methods

Materials and Instruments

The Irish *Fucus vesiculosus (Fucus v.)* alga was collected in July 2016 from the intertidal shore of the Stratford Lough, Belfast, Northern Ireland, (UK) at N 54º 26' 40 and W 05º 35' 40 of the Irish Sea with a salinity of 35 ppt. The algae material was washed with DI water, sliced in 2-3 cm size cuttings and dried, before being tested as a bio-sorbent in adsorption experiments. All chemicals used in this work were Sigma Aldrich high purity grade [($Cd(NO_3)_2 \cdot 4H_2O$ (CAS # 10022-68-1), $CdCl_2$ (CAS # 10108-64-2), $C_4H_6CdO_4$ (CAS: 543-90-8), NaOH (CAS # 1310-73-2), HCl (CAS # 7647-01-0) and EDTA (CAS # 60-00-4), CH_2-COONa, Na alginate, ALG, (CAS: 9005-38-3), (CH_2-COO) Na – Na carboxymethyl cellulose, CMC, (CAS: 9004-32-4)]. Organic mixtures such as $(C_6H_7O_6)_2Cd$ = Cd(II) alginate and $(CH_2\text{-}COO)_2Cd$ = Cd(II) carboxymethyl cellulose (CMC) were synthesized by mixing 10% ALG and 2% CMC with 5 mM Cd nitrate solution. Cd foil, $CdCl_2$, $Cd(NO_3)_2$, $C_4H_6CdO_4$, $CdSO_4$, and boron nitride, BN (10043-11-5) as well as the synthesised Cd(II) organic mixtures were used as standards and reference materials for spectroscopy measurements and as well as to aid data processing and interpretation.

For adsorption experiments, we used a pH stat Titrator (SI Analytics7000) which aids to maintain a constant pH for the duration of the experiments by continuous monitoring of the pH, and the addition of specific volumes of either acid or base as necessary. A multi-element lamp Flame Absorption Atomic Spectrometer (FAAS) (FAAS ContrAA 300) was used to measure Cd(II) concentrations from supernatant solutions after sorption experiments. A Field Emission Gun Scanning Electron microscope (CANSCAN Scanning Electron Microscope) was used to collect images from the algae tissue before

and after exposure to Cd(II) solutions. A micro–Fourier Transform Infrared (FTIR) bench top spectrometer (Nicolet 6700 Thermo equipped with a Smart Orbit ATR and a diamond window) was used to collect infrared spectra of untreated algae sample (blank) and algae samples after sorption experiments at various Cd(II) concentrations and pH values. Synchrotron micro–X-ray Fluorescence spectroscopy (XRF) and X-ray Absorption Spectroscopy (XAS) analyses were performed on the I18 beamline at Diamond Light Source.

A series of software such as Origin pro (OriginLab, 2007), Geochemist Workbench (Bethke, 2002) and Athena from Demeter Strawberry Pearl package (Ravel and Newville, 2005) were used for data plotting, adsorption kinetics and equilibrium isotherms modelling and statistics; geochemical modelling and liner combination fitting spectroscopy data processing, respectively.

Cd(II) geochemistry in solution

The speciation of Cd(II) in solution was calculated and plotted at working concentrations of 1 and 10 mM using the geochemical modelling software, Geochemist Workbench (Bethke, 2002). We used *thermos.vdb* (thermodynamics), *comp_2008.vdb* (components) and *type6.vdb* (solids) databases for the modelling as they contain the relevant parameters and constants for Cd(II) compounds evaluated at the conditions of this work and they are referenced by National Institute of Standardization (NIST).

Adsorption experiments

Effect of pH and Cd(II) concentrations

To investigate the effect of pH and Cd(II) concentrations on Cd(II) adsorption onto *Fucus v.,* the experiments were performed under dynamic regime assured by a magnetic stirring at 150 rpm for 180 min in 100 mL solution, in 125 mL reaction vessel that simulates a batch reactor. Dried algae samples were used in all the experiments at three different pH values (5, 7 and 9) and at room temperature (~21°C). 1 g of dried algae L^{-1} was allowed to interact with 1 mM Cd(II) nitrate solution at different pH values to evaluate the effect of pH, and at concentrations of Cd(II) nitrate between 1 mM and 10 mM nitrate to investigate the effect of concentration. The pH was continuously measured and maintained constant with the potentiometric titrator (SI Analytics7000) by adding either acid (HCl, 10 mM) or base (NaOH, 1M, 100 mM, and 10 mM) in volume steps of 0.01 mL as needed. The Cd(II) solution at 10 mM had an initial pH of 5.8, while that at 1 mM had a pH of 6.3. Aliquots of 5 mL were taken at various time

series, filtered through 0.45 µm cellulose nitrate membranes, acidified and prepared for Cd(II) analysis by FAAS with a detection limit of 0.5 mg L^{-1}. Adsorption experiments as a function of pH were performed in triplicates to meet the requirements of statistically relevant number of samples, and for which a standard deviation was calculated below 5%. Blanks (algae in solution with no Cd(II)) were included to check whether Cd(II) is originally present in the algae habitat, and to find out the buffering capacity of the algae during the adsorption experiments.

Eluent for Cd(II) desorption, algae functionalization, and reuse in repetitive cycles

Adsorption experiments for Cd(II) desorption, algae functionalization and reuse in multiple cycles were performed in a rotary mixer (Biosan Multi Bio SR-60) under a dynamic regime using 1g L^{-1} of biomass and a fixed volume of 50 mL of eluent. For cyclic adsorption studies a solution of 10 mM Cd(II) was used. Sacrificial replicates were performed for each eluent type, and we run experiments in triplicate to evaluate the reuse of biomass. The supernatant solution was filtered after experiments and prepared for FAAS analysis. A sacrificial algae sample from consecutive sorption cycle, before desorption, was kept for FTIR spectroscopic characterization and synchrotron XRF and XAS measurements.

Adsorption kinetic modelling

Experimental kinetic profiles were fitted to chemical reaction-based models such as pseudo first order (PFO)(Lagergren, 1886), pseudo second order (PSO) (Ho, 2006; Ho and McKay, 1998) kinetic models, Elovich model and Webber Morris – intraparticle diffusion (W-M) kinetic model (Anastopoulos and Kyzas, 2015; Azari et al., 2019; Azari et al., 2017; Brinza et al., 2009; Kumar et al., 2016; Kumar Yadav et al., 2018) (Table SI 1). Best fits were evaluated as highest R^2 value and the lowest chi-square, χ^2.

For Cd(II) desorption, solutions of 10 mM HCl and NaOH and 1mM EDTA were used as individual eluents aiming to functionalize and regenerate the biomass which would allow us to use this biomaterial in multiple adsorption cycles. A volume of 50 mL eluent per 0.05 g (to yield a concentration of 1gL^{-1}) of biomass were mixed in a rotary mixer (Biosan Multi Bio SR-60) for 2 hours. Statistically relevant replicates (at least three) were desorbed in 50 mL of HCl (10 mM), NaOH (10 mM) and EDTA (1 mM - solubility did not allow use of higher concentration) for 30 minutes. The solids from the sacrificial

replicate recovered from each experiment set were kept for characterisation and synchrotron analyses (i.e., FTIR, XRF and XAS). 5mL of supernatant from all replicates were filtered, acidified and analysed for Cd(II) by FAAS. At the start of the second adsorption cycle, the pH of the solutions was for HCl (4.1), NaOH (5.0) and EDTA (5.5).

Adsorption isotherms

Batch systems were used for the adsorption isotherms experiments using $10gL^{-1}$ of algae concentration and concentrations of Cd(II) between 10 µM and 10 mM. The adsorption isotherms data were plotted as uptake capacities versus Cd(II) concentration at equilibrium. The modelling was performed by using Langmuir (Langmuir, 1916) and Freundlich models (Azari et al., 2015; Azari et al., 2019; Azari et al., 2017). The models are presented and described in the SI. Briefly, both models are theoretical and / or empirical expression of adsorption equilibrium, and they involve various assumptions used to derive indirect mechanistic information but they can be used to obtain and compare adsorption capacities of various adsorbents for specific adsorbates or of various adsorbates for the same adsorbent, under similar or ideally identical process conditions (Al-Ghouti and Da'ana, 2020; Ayawei et al., 2017), (Azari et al., 2020).

Algae characterization

Algae surface was imaged after adsorption experiments using a CANSCAN Scanning Electron Microscope (SEM) at 20 keV. Identification of mineral precipitates formed in the experiments at pH 9 was performed using a Shimadzu X-ray diffractometer (XRD) (Cu K_α radiation at 40 kV, and 30 mA, scanning range 10 - 90 theta, scan speed 2 degree min^{-1}, step size 0.02 degrees). Evaluation of diffraction patterns and identification of the Cd(II) phase present was performed using the Joint Committee on Powder Diffraction Standards (JCPDF) database (Otavite, R050677-1).

To quantify the spatial distribution of Cd(II) adsorbed onto the algae surface, we performed X-Ray Fluorescence (XRF) mapping on I18 microfocus beamline at Diamond Light Source, UK. I18 uses a Si (111) monochromator and Kirkpatrick-Baez mirrors for focusing the beam on the sample and two silicon mirrors were used for the rejection of higher order harmonics. For the analyses, algae samples removed immediately after adsorption experiments were analysed without further treatment. Small sections (~ 5x5 mm^2) of algae were mounted on sapphire discs and placed on a cryostat holder (Microstat HiResII, Oxford Instruments), which maintained the samples at 10 K to prevent any radiation damage during the

measurements. To avoid absorption of the low fluorescence energy signal in air, the samples were kept in a helium environment in which the cryostat and detector were enclosed. Maps covering areas of circa 200 x 200 μm^2 were collected from different parts of the algae surface with a resolution of 3 µm and dwell time of either 0.5 or 1.5 sec per point. A 4-channel Vortex detector was used at 45° geometry and the excitation energy was 5 keV. Cd(II) was identified by the fluorescence lines $L_{\alpha 1}$ at 3133 eV, $L_{\beta 1}$ at 3315 eV and $L_{\beta 2}$ at 3526 eV. XRF data were processed and displayed in PyMCA software which allowed deconvolution of fluorescence peaks to overcome the partial overlap with K peak.

Local bonding environment of Cd(II) onto or within bio matrices was quantified by X-ray Absorption Spectroscopy (XAS). X-ray Absorption Near Edge Spectroscopy (XANES) scans were collected between 3400 eV and 3510 eV with an energy step of 5 eV and acquisition time of 1s; then between 3510 eV and 3530 eV, an energy step of 1 eV and acquisition time of 1 sec was used; between 3530 eV and 3570 eV, an energy step of 0.3 eV and acquisition time of 3 sec were used; between 3570 eV and 3650 eV, the data were collected using an energy step of 1eV and acquisition time of 1s; and finally continued with an energy step of 2 eV and acquisition time of 1 sec to the final energy of spectra, 3730 eV. The beam size for XANES analysis was 3 µm. Spectra were collected on areas of high, medium, and low Cd(II) concentrations selected from the XRF maps at points of interest (POI) where K was absent. Spectra from Cd(II) organic (i.e., $(C_6H_7O_6)_2Cd$=Cd alginate and $(CH_2\text{-}COO)_2Cd$ = Cd(II) carboxymethyl cellulose) and inorganic (i.e., $CdCl_2$, $Cd(NO_3)_2$, $C_4H_6CdO_4$) standard species were also collected to aid with data interpretation. XANES spectra were background subtracted, normalized and processed in Athena for direct comparison or linear combination fitting (LCF).

FTIR spectroscopy was used to identify organic functional groups on the algal surface by detecting vibration frequencies and their possible shifts before and after Cd(II) adsorption using wet algal tissue. 512 scans per spectra were recorded in the mid-infrared range from 4000 to 600 cm^{-1} at a resolution of 4 cm^{-1} using a Nicolet 6700 Thermo Scientific bench top spectrometer with a Smart Orbit ATR using a diamond window. The FTIR spectra from standards were also collected as mentioned in material section.

Results

Cd(II) speciation in solution

To understand the processes and mechanisms of Cd(II) adsorption in a bioprocess, it is important to understand its chemistry in aqueous media before reacting it to the algal surface. Therefore, the geochemical modelling package was used to provides fundamental information about Cd(II) species that are stable under specific pH and concentration conditions. Figure 1 shows Cd(II) speciation in solution as a function of pH and concentration under standard conditions (1 atm and temperature of 25°C).

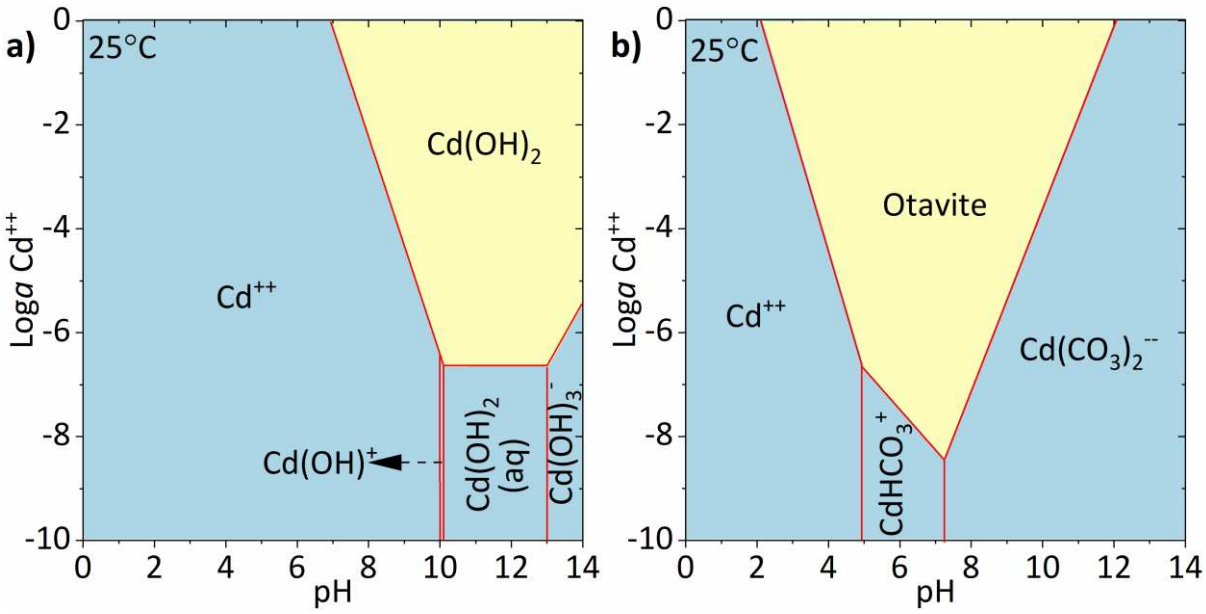

Figure 1. Cd(II) speciation in solution in the absence (a) and the presence (b) of CO_2 (from the atmosphere), expressed as a function of pH and logarithmic activity of Cd^{2+} ions, calculated in Geochemist Workbench software (Bethke, 2002).

Under ideal conditions at low concentrations of Cd(II), acidic pH in a closed system (no interaction with air and other ions), Cd is essentially found in solution as divalent ion (**Figure 1**). At pH above 10 and concentrations below ca. 10µM (log a Cd -7), Cd(II) can form hydroxylate aqueous species positively (from pH 10 to 10.2), neutral (from pH 10.2 to 13) and negatively (above pH 13) charged. However, as Cd(II) concentration increases in solution, the saturation of Cd(II) ions occurs, and precipitation initiates. In the current diagram, $Cd(OH)_2$ is an example of mineral which can form by ions when the saturation in solution is reached. In the particular case of a system that is equilibrated with CO_2 from the atmosphere, otavite, $CdCO_3$ is the most stable specie (**Figure 1 b)**. Obviously, this information can be only used as a guidance because in real systems the occurrence of simultaneous process (i.e., desorption of light ions, ion exchange from sorbent surface) will generate a mixture of Cd species. In addition, the presence of ions from seawater (Brinza et al., 2009) or those naturally present

in the algae, increases the complexity of the system changing the activity coefficient of each ion and therefore modifying the sorption capacity (Moreira et al., 2019). On the other hand, it was noted, that the Geochemist Workbench software uses databases that in some cases contain non standardized parameters and constants or incomplete for certain conditions (i.e., temperature and pressure). It is therefore recommended to check the databases before using them as the model can yield inconsistencies in the Cd(II) species found even when using the same database. An example of these inconsistencies is shown in (**Figure SI 1**). It is also advisable to check more databases and their inputs for specific species and compounds and use those referenced by NIST. In addition, in practice for real application purposes, geochemical simulation of ions speciation in solution can be computed considering the elemental analyses of polluted water which need to be treated or depolluted. As opposed to other metals in a simple ideal system, i.e. Zn, from the above diagrams it is observable that Cd is found as free bivalent ion in solution over a larger pH interval. This may also impact on the adsorption capacities (positive effects in CO_2 free systems such as column type reactors and negative effects in open systems such as batch reactors, potentially used for adsorption process) over a large pH interval.

Effect of pH and initial concentration on Cd(II) adsorption

Kinetic profiles of Cd(II) adsorption onto *Fucus v.* as a function of pH and initial concentration of Cd(II) using four most popular kinetic models (i.e., PFO, PSO, Elovich and Webber –Morris intra-particles diffusion model) are shown in **Figure 2**. They show that the adsorption of Cd(II) onto dried algae takes place relatively fast, reaching a steady stage after two hours; the weighted Cd(II) uptake capacity of *Fucus v.* at the three pH values studied were similar (pH 5, 0.547±0.020 mmol g^{-1} ; pH 7, 0.610 ±0.044 mmol g^{-1} and pH 9, 0.512 ±0.035 mmol g^{-1}) **(Figure 2a)**. Considering the dissociation constants for short-chained carboxylic acids ($4<pK_a<6$) and hydroxyl groups and $9<pK_a<11$) it may be interpreted that adsorbed Cd(II) at low pH is mostly associated with carboxylic groups, while at high pH, the non-precipitated Cd(II) ions could mostly be bind to hydroxyls groups (Fang et al., 2011).

Varying the initial concentration of Cd(II) from 1 to 10 mM at pH 5, increased two times the concentration of Cd(II) adsorbed onto algae surface (1.019 ± 0.057 mmol g^{-1}) **(Figure 2b)**. In addition, the higher concentration of Cd(II) allowed to reach faster (1 h) the steady state of adsorption, indicating a faster saturation of adsorption sites on the algae surface. It should be noted that Cd(II) precipitated in the solution at pH 9 and therefore, not all the Cd(II) separated from solution can be accounted as

adsorption. Cd precipitate formed at pH 9 was filtrated and identified by powder diffraction as otavive, $CdCO_3$ (see **Figure SI 2**).

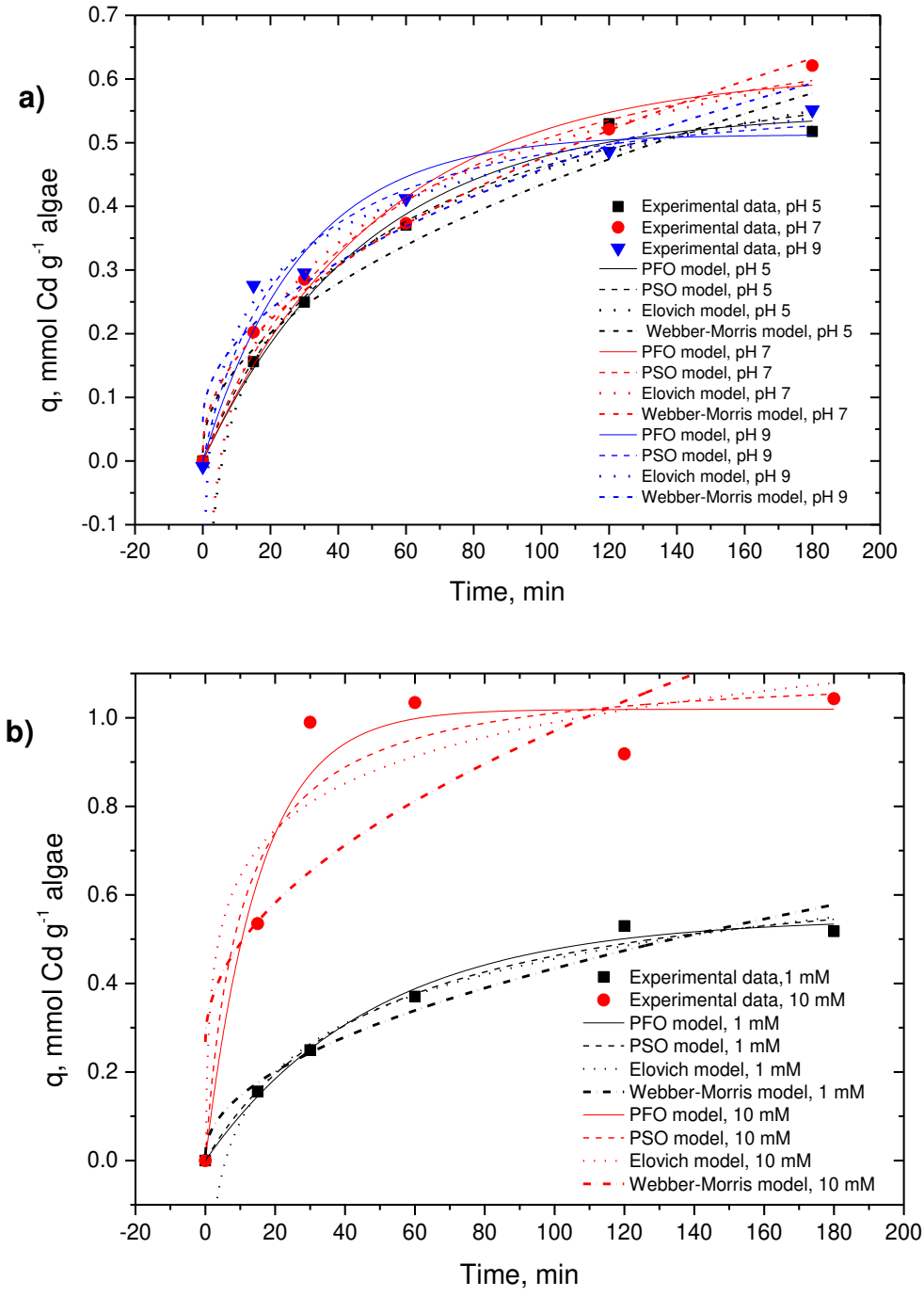

Figure 2. Cd(II) adsorption profiles onto dried *Fucus v.* at pH 5, 7 and 9 (a); and for 1mM Cd(II) and 10 mM Cd(II) (b), including kinetic fits to pseudo first order (straight line), pseudo second order (discontinued line), Elovich (dotted line) and Webber-Morris (alternating line and dot line) kinetic models.

Adsorption kinetics and equilibrium isotherms modelling

Adsorption kinetics

Depending on pH, our data fit better to different adsorption models (see Table 1). At pH 5, the best fit was achieved using the PFO kinetic model (Adj. R^2 = 0.9912), while at pH 7 the fit was better achieved using the Webber Morris model (Adj. R^2 = 0.9961); and at pH 9, a good fit was obtained using the Elovich model (Adj. R^2 = 0.9863). This may suggest a change in sorption mechanism as a function of pH and Cd(II) concentration. For experiments at pH 5 and for both Cd concentrations, 1 mM and 10 mM, the weighted values of q_e at equilibrium, derived from PFO model fits (0.547 mmol g^{-1} and 1.019 mmol g^{-1}) are in good agreement with the experimental data (0.517 mmol g^{-1} and 1.04 mmol g^{-1}) fact that confirms the effectiveness of the model chosen.

According to our results at low pH (5) and concentrations between 1 mM and 10 mM Cd, Cd(II) adsorption on the surface of *Fucus v.* is predominantly a physical mechanism (PFO kinetic model) based on weak interactions such as hydrogen bonds or Van der Walls forces (Kumar et al., 2016; Vafajoo et al., 2018; Zeraatkar et al., 2016). These interactions were suggested to occur rapidly as a function of metal concentration, presumably in excess, but they were limited to the available adsorption sites on the algae surface leading to a rapid saturation as the concentration increases (Hubbe et al., 2019; Qiu et al., 2009). However, our fit results to the PSO kinetic model (Adj. R^2 = 0.9861 for C_{Cd} 1 mM and Adj. R^2 = 0.9127 for C_{Cd} 10 mM at pH 5) indicate that besides physical sorption, a chemical adsorption may also take place to a certain extent involving covalent bonding, particularly as Cd(II) concentration increases.

At neutral pH, the mechanism for Cd(II) adsorption is likely the diffusion through the thick hydrated layer of the interface from solution to algae surface sites (Webber-Morris kinetic model), which was quantified through potentiometric titration as being significant due to the fact that the pH value of zero charge of *Fucus v.* is near the neutral (Brinza et al., 2019; Brinza et al., 2009). This would be the limiting step of the adsorption process. Good fits were obtained at neutral pH to the Elovich model (Adj. R^2 = 0.986) and the PSO kinetic model (Adj. R^2 = 0.984), indicating a possible chemisorption mechanism in the system, involving strong chemical bonding such as ionic and covalent bonds.

Table 1. Summary of fitting parameters of the kinetic profiles modelling with the Pseudo-First Order, Pseudo-Second Order, Elovich, Webber Morris Kinetic Models.

Kinetic profiles modelling parameters					
System	**Parameters and statistics**	**PFO model**	**PSO model**	**Elovich model**	**W-M diffusion model**
pH 9, C_{Cd} 1mM		q_e = 0.51 ± 0.035 k_1 = 0.034 ± 0.007	q_e = 0.596 ± 0.041 k_2 =0.07 ± 0.0219	α = 0.066±0.0176 β = 8.624± 0.864	k_{id} = 0.039± 0.0051 C = 0.061 ± 0.042
	Red. X^2	0.0023	0.0011	5.441E-4	0.00315
	Adj. R^2	0.942	0.971	**0.986**	0.921
pH 7, C_{Cd} 1mM		q_e = 0.61 ± 0.04 k_1 = 0.018 ± 0.003	q_e = 0.777 ± 0.059 k_2 =0.023 ± 0.006	α = 0.032±0.004 β = 5.983± 0.470	k_{id} = 0.045± 0.0013 C = 0.016 ± 0.010
	Red. X^2	0.0016	8.009E-4	6.962E-4	1.904E-4
	Adj. R^2	0.968	0.984	0.986	**0.996**
pH 5, C_{Cd} 1mM		q_e = 0.547±0.020 k_1 = 0.020±0.002	q_e = 0.70±0.049 k_2 = 0.027±0.007	α = 0.027±0.003 β = 6.253±0.555	k_{id} = 0.042 ± 0.004 C = 0.012 ±0.034
	Red. X^2	3.807E-4	6.027E-4	8.129E-4	0.00207
	Adj. R^2	**0.991**	0.986	0.981	0.952
pH 5, C_{Cd} 10mM		q_e =1.019±0.057 k_1 = 0.064 ± 0.015	q_e = 1.112 ± 0.111 k_2 = 0.089 ± 0.055	α = 1.061 ± 2.613 β = 6.623 ± 3.224	k_{id} = 0.070 ± 0.024 C = 0.267 ± 0.198
	Red. X^2	0.0088	0.0150	0.0218	0.0692
	Adj. R^2	**0.948**	0.912	0.873	0.598

Note: q_e (mmol g^{-1}); k_1 (min^{-1}); k_2 (g $mmol^{-1}$ min^{-1}); α (mmol g^{-1} min^{-1}); β (mmol g^{-1} mg^{-1}); k_{id} (mmol g^{-1} $min^{-1/2}$)

Several studies have combined kinetic models and interpret metal adsorption data onto *Fucus v.* from other places around the world (Ahmady-Asbchin and Jafari, 2013; Brinza et al., 2019; Brinza et al., 2020; Brinza et al., 2009; Castro et al., 2017; He and Chen, 2014; Henriques et al., 2017; Mata et al., 2009). Most of the studies on metal adsorption onto brown algae, including *Fucus v.*, have obtained good fits to the PSO kinetic model (He and Chen, 2014; Herrero et al., 2006; Lodeiro et al., 2005; Mata et al., 2009). A study investigating Cd, Ni and Pb adsorption onto *Fucus v.,* collected from a Brazilian farm, obtained a good fit to the Elovich kinetic model compared to the W-M intraparticle diffusion model (R^2 = 0.999), the Pore and surface mass diffusion model (R^2 = 0.997), and the PSO kinetic model (R^2 = 0.996). Based on the desorption constant of this model, the authors suggested that the algae surface had a greater affinity to adsorb Cd(II) than Pb. Additionally, based on these results, they suggested that adsorption followed a diffusion-controlled mechanism and that particularly, the main contributor to the biosorption process was the diffusion boundary layer. They concluded that external transport of the metal was directly affected by particle size of the bio sorbent, in their case at the scale of microns (Moreira et al., 2019). The discrepancy of the results in similar experiments lies on the different conditions used (e.g., biomass type, habitat, preparation, metabolism stage, time of collection, etc), as well as the chemistry of the solution (e.g., metal source type/salt and the presence of counter and competitive ions), both of which have a direct impact on the chemistry of the algae surface (Brinza et al., 2005, 2007; Kumar et al., 2016; Kumar Yadav et al., 2018).

Adsorption isotherms

The experimental data yielded a better fit to the Langmuir isotherm (R^2= 0.994) compared to the Freundlich isotherm (R^2 = 0.953) (**Table 2** and **Figure 3**). The calculated positive parameter (RL) indicated that adsorption is favourable and that the adsorption may occur as a monolayer with a maximum uptake capacity of 1.203 mmol g^{-1}. Comparing our data with the maximum Cd(II) uptake capacity reported for other brown algae from various places around the world (i.e., Spanish Ca pre-treated *Sargassum muticulum* (0.45 mmol g^{-1}); Chilean *Lessonia nigrescens* (0.32 mmol g^{-1}) and *Durvillaea antartica* (0.4 mmol g^{-1}) as compiled in a recent review by Mazur et al. (Mazur et al., 2018), the Irish algae *Fucus vesiculosus* is a very good sorbent for Cd, placing it close to or above species like *Sargassum muticum* and *Laminaria japonica* (Mazur et al., 2018)*, or* other *Fucus species* such as *Fucus Serratus* (Ahmady-Asbchin et al., 2008) or even the same species, *Fucus v.* from various places around the world (Ahmady-Asbchin and Jafari, 2013; Mata et al., 2009; Mata et al., 2008) (see **Table SI 2**).

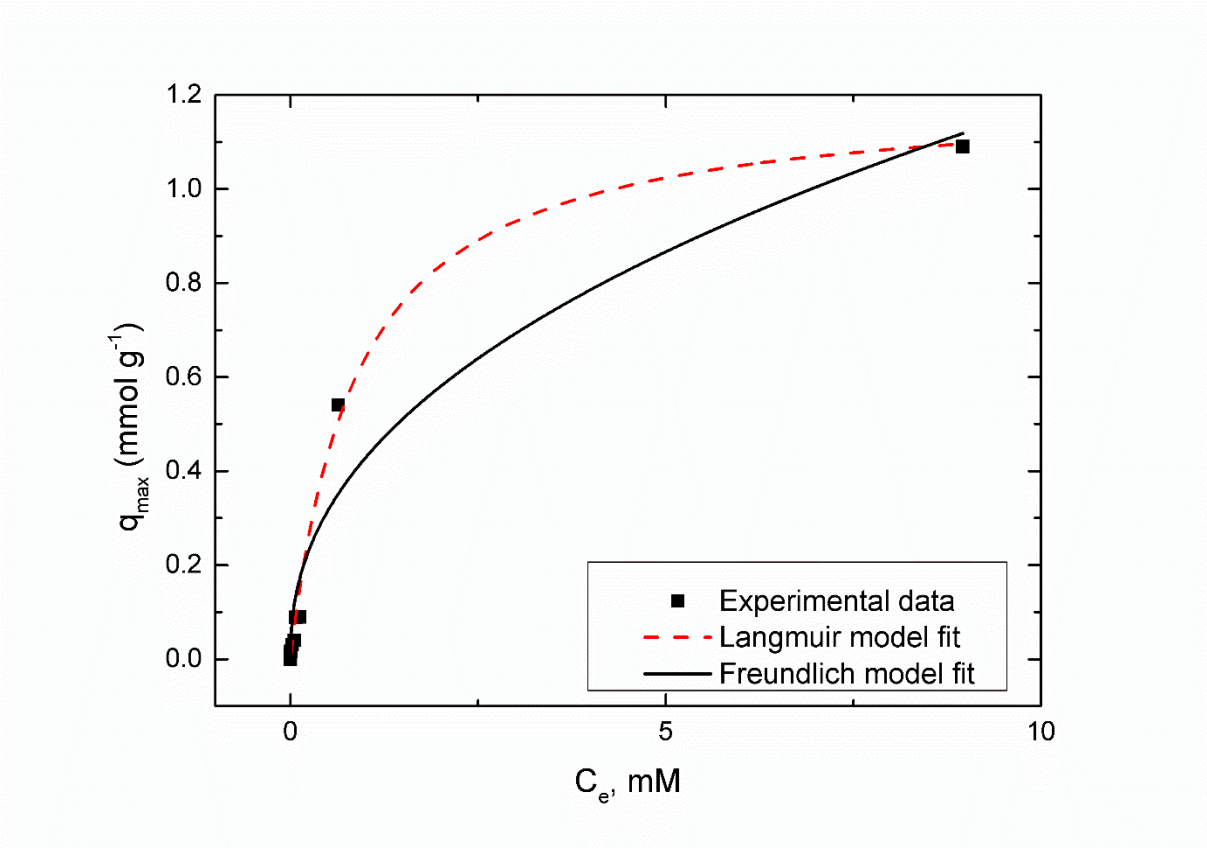

Figure 3. Cd(II) a**dsorption isotherms modelling** with the Langmuir and Freundlich Models

Table 2. Summary of fitting parameters from a**dsorption isotherms modelling** with the Langmuir and Freundlich Models.

	Langmuir isotherm	**Freundlich isotherm**
Parameters	q_{max} = 1.203±0.035 mmol g^{-1} b = 1.143±0.116	K_f = 0.428 ±0.047 mmol g^{-1} n = 2.28 ±0.27
	R_L=0.08045	
Statistics	Adj. R^2 = 0.994 R^2 = 0.995 Red. X^2 = 0.0007082	Adj. R^2 = 0.948 R^2 = 0.953 Red. X^2 = 0.0063

A comparison of our results with previous studies on green, red and brown algae, which found the maximum Cd(II) uptake within the range 0.5 -1.17 mmol g^{-1} at pH values between 4.0 and 5.5 (He and Chen, 2014), classes our Cd(II) adsorption results on the Irish *Fucus v.* (1.203 mmol g^{-1}) as superior. As examples, Cd(II) uptake capacity onto Spanish *Fucus v.* (Pontevedra, Spain) has been reported to be 0.9 mmol g^{-1} at pH 6.0 in experiments using a biomass concentration of 0.5 g L^{-1} that was washed, pre-treated with $CaCl_2$, dried and grinded to powder (Mata et al., 2008). Other works using different *Fucus* species from different habitats have reported uptake capacities values for *Fucus serratus* (0.72 mmol g^{-1}), *Fucus v.* (0.79 mmol g^{-1}, 0.85 mmol g^{-1}), *Fucus Ceranoides* (0.65 mmol g^{-1}), indicating that the Irish kelp has a better efficiency for Cd(II) uptake. However, differences in algae habitat, experimental preparations, and process conditions can explain some of the above variations (Brinza et al., 2019; Brinza et al., 2020; Brinza et al., 2009; Herrero et al., 2006).

Comparing the current Cd(II) quantitative results for the Irish *Fucus v*, with our previous results on Zn uptake by same algae specie it can be noticed that the Irish kelp is a better bio sorbent (as referred to the uptake capacity at pH 5 under same process conditions, which is four times higher) for Cd(II) than for Zn (Brinza et al., 2019) over a wider pH interval.

In contrast to other low cost adsorbents currently explored (e.g., activate carbon, walnut shell, rice husk, oak bark, chestnut bur, banana peels, mandarin peel, tea waste, maple leaves, coffee grounds, sunflower plants), which have a maximum Cd(II) uptake capacity of 0.22 mmol g^{-1} (Pyrzynska, 2019), *Fucus vesiculosus*, is an efficient and effective low cost reusable adsorbent. All the above comparisons enhance the feasibility of the selected algae specie as a highly potential green by-product for its application to clean bio technologies used for metals uptake from polluted waters.

Cd(II) adsorption – effect of desorption eluent types and biomass reuse in repetitive cycles

409 **Figure 4** shows the results of desorption experiments from multiple adsorption cycles using
410 HCl, NaOH and EDTA**.** It can be observed that regardless the eluent used, the algae uptake efficiency
411 increases in the second cycle, being the maximum absorption, before decreasing substantially**.** The
412 uptake capacity of Cd(II) onto *Fucus v.* from four adsorption repetitive cycles using 10 mM HCl is shown
413 in **Figure 4a**. On the first cycle, the Cd(II) adsorbed onto dried algal biomass was ~ 2.15 mmol g^{-1} and
414 increased to 2.88 mmol g^{-1} on the second cycle. This indicates that HCl induced Cd(II) desorption likely
415 through the protonation of the sites on the algae surface. On the third cycle, the uptake capacity
416 substantially decreased to 1.6 mmol g^{-1} (~ 60%) and this behaviour continued on the fourth cycle to 0.5
417 mmol g^{-1} dried algae. The increasing uptake capacity in the second and the third cycle as compared to
418 the maximum uptake capacity obtained for the Irish kelp suggest that the use of HCl, beside metals
419 elution, also clean and protonate the algae surface, increasing the amount of sites suitable and available
420 for Cd(II) bounding. The decreasing Cd(II) loading on the third cycle results indicate that HCl at the
421 concentration used in this work, likely caused biomass degradation, further suggesting future tests using
422 lighter concentrations of acid.
423 When NaOH was used as an eluent, ~ 1.5 mmol g^{-1} dried algae remained adsorbed (~30% less
424 than HCl) after the first adsorption cycle (**Figure 4.b**). On the second cycle Cd(II) was quantified as
425 twice as much as in the first cycle, precisely 3.2 mmol g^{-1} dried algae. In the third and the fourth cycles,
426 Cd(II) adsorbed was ca 2 ± 0.1 mmol g^{-1} dried algae, which could be considered very good as compared
427 to the first (ca 25% more) and the second (ca. 30% less) cycles. Cd(II) elution by NaOH, might have
428 occurred by microprecipitation and desorption. It is to be noted that for the NaOH system, the efficiency
429 of adsorption in the adsorption-desorption cycles after the first, is the highest among the three eluents
430 chosen. However, these superior values should be interpreted cautiously by considering the fact that
431 they include the microprecipitation which was not quantified separately in this study.

432 The use of 1 mM EDTA was found to be a good concentration to desorb Cd(II) while
433 regenerating the biomass. After the first cycle, Cd(II) was adsorbed ca. 1.4 mmol g^{-1}, similar to that when
434 using NaOH (**Figure 4c**). The biomass uptake capacity increased considerably with up to 2.85 mmol g^{-1}
435 , similar value with that from using HCl. The decrease of Cd(II) sorption capacity in the third and fourth
436 cycles was relatively significant lower (1.5 ± 0.2 mmol g^{-1}) in comparison to the NaOH and HCl systems.
437 These results indicate that EDTA does not degrade the algal tissue at the same extent as HCl in the
438 fourth cycle, and provides a great functioning (such as CH_2 and -COOH) of the bio sorbent surface that

ensured significantly more Cd(II) uptake in further cycles and biomass reuse, as opposed to Cd(II) maximum uptake capacity obtained from thermodynamic isothermal studies.

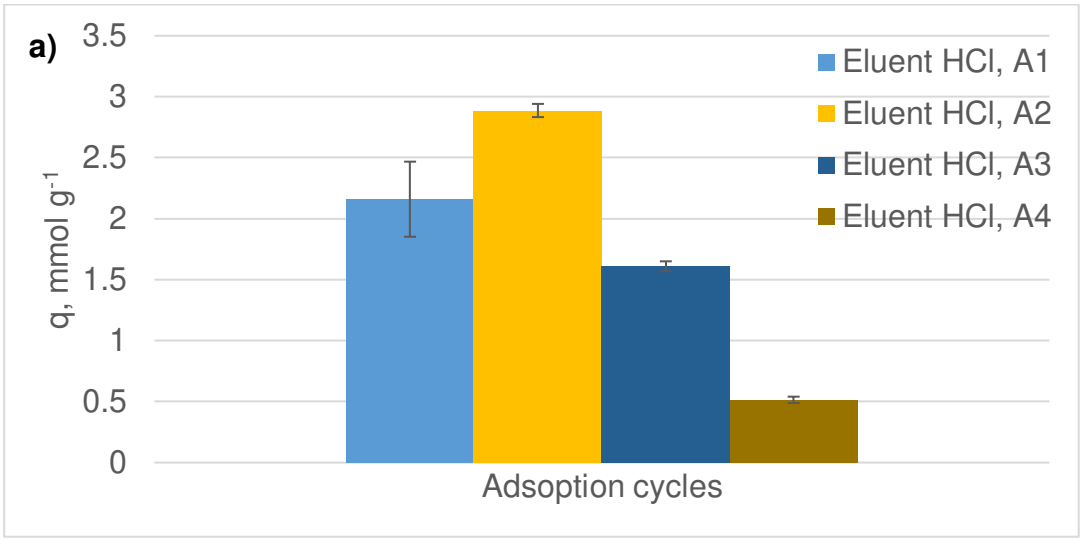

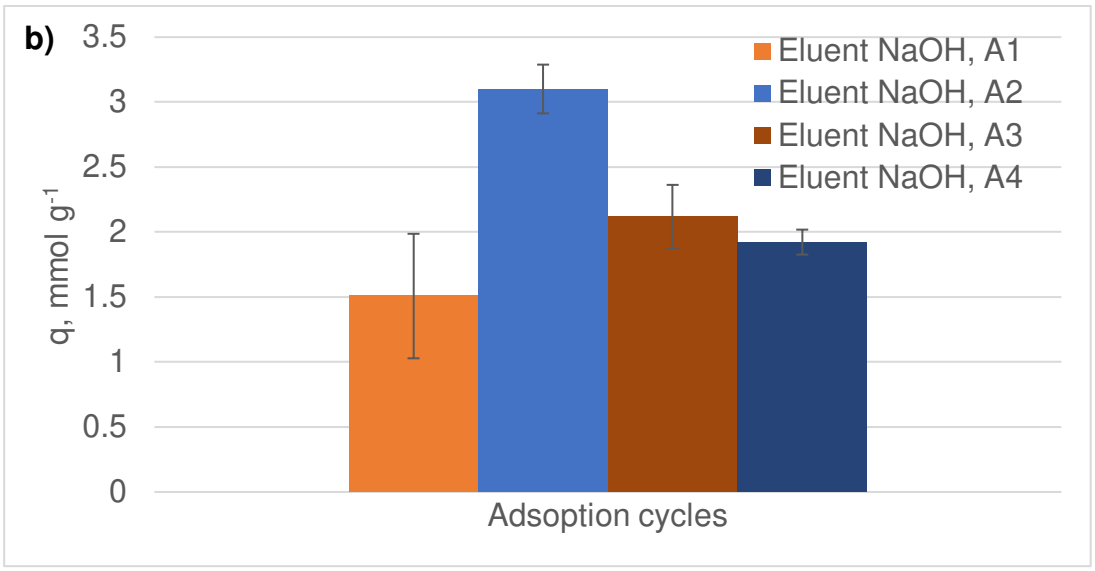

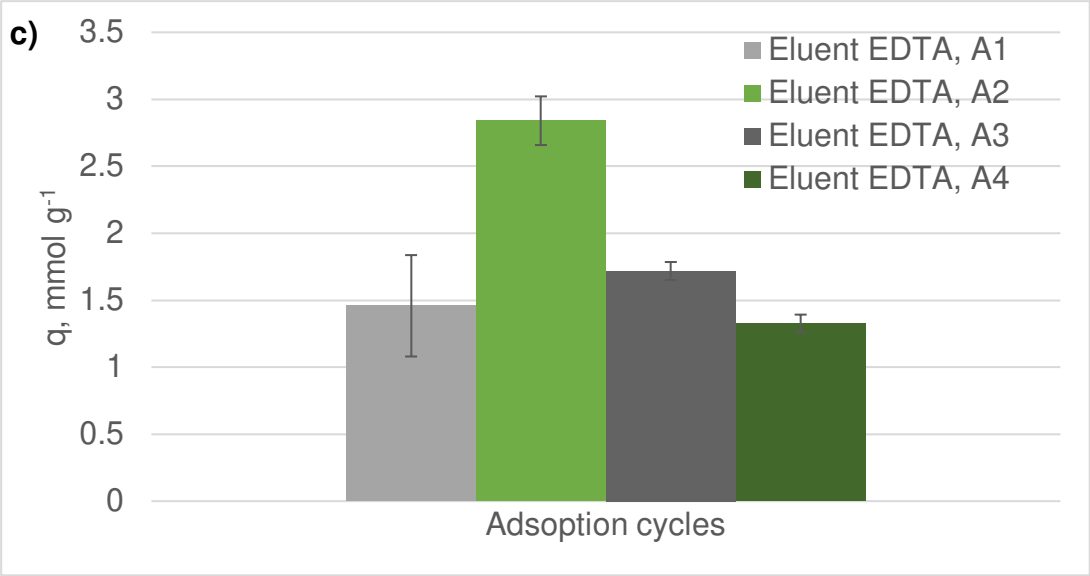

Figure 4. Uptake capacity of Cd(II) onto *Fucus vesiculosus* from 4 consecutive adsorption – desorption cycles (labelled A1-A4) using as eluent (a) HCl; (b) NaOH and (c) EDTA.

Only few studies are currently available in the literature regarding the reuse of algae biomass for pollutant uptake applications, and reports about eluent types are scarce. A recent study looking at the uptake capacity of the brown algae, *Sargassum muticulum,* for methylene blue dye and Pb(II) from polluted water in column tests reported good performance in up to five adsorption-desorption cycles performed. Another work investigated Cu(II) adsorption on the brown macroalgae specie, *Ascophylum nodosum*, using HCl and $CaCl_2$ in multiple cycles at various concentrations in both batch and column experiments. This work reported that high efficiency of Cu (II) elution is achieved when using 3% HCl for up to four cycles without damaging the biomass (Mazur et al., 2017). Another study on Cu desorption from the marine green algae, *Helimeda gracilis*, found that 200 mM HCl solution desorbed up to 98% of the Cu(II) adsorbed on the algal surface (Jayakumar et al., 2015). This would indicate that lower concentrations of HCl could be used for the desorption of Cd(II) from *Fucus v.* but this needs to be tested in future experiments.

Algae characterization

SEM images of algae talus tissue at a scale from 100 to 3 microns are presented in **Figure 5**. A wrinkled pattern of 10 - 20 microns in size is observed in **Figures 5a - 5f**. These patterns were enhanced by the process of algae drying as the images were acquired under vacuum; they show the cellulose fibres forming the algae tissue. These fibres are also observed in the transversal sections of the algae **(Figures 5g – 5i),** thallus also showing Cd(II) precipitation (~ 2-5 µm) as was observed onto the algae

surface. This indicates that solutions with Cd(II) at concentrations >10 mM precipitates, besides the uptake by the algae. The presence of the precipitates seen are supported by the geochemical modelling results displayed in **Figure 1b**.- that indicates the formation of otavite precipitate in open systems equilibrated with atmospheric CO_2.

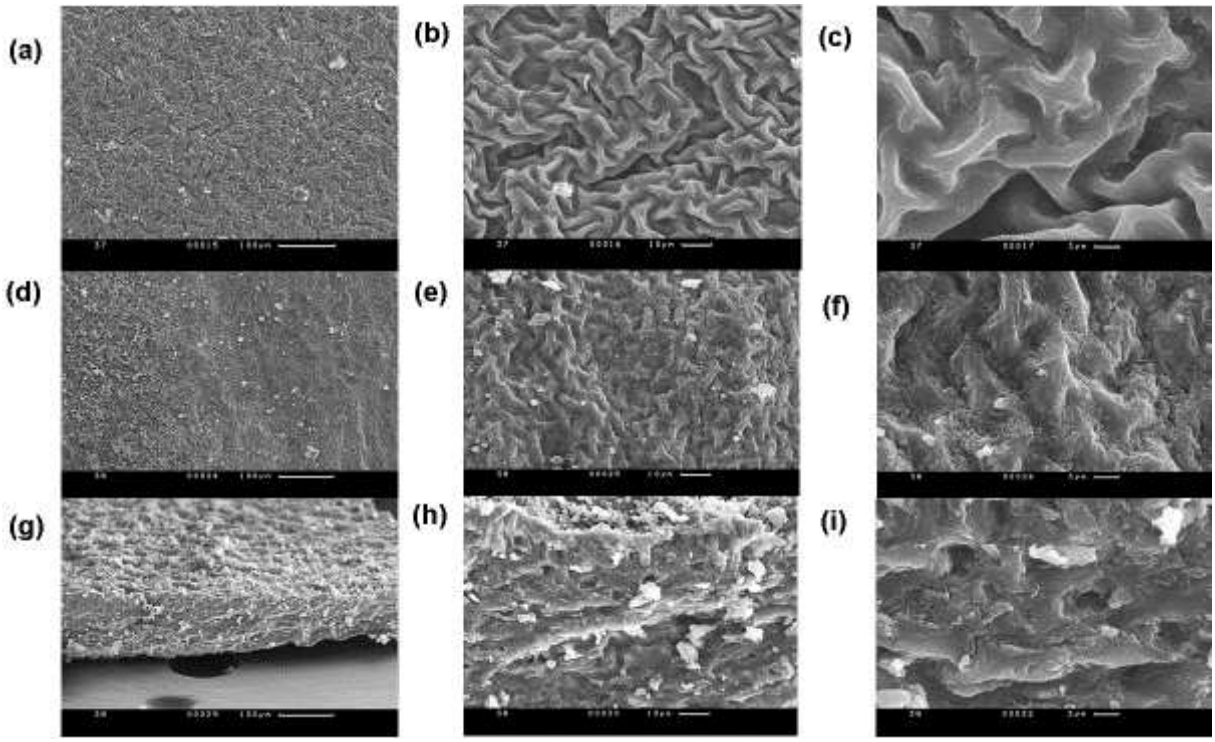

Figure 5. SEM micrograpfs of sections of *Fucus v.* before (a), (b) and (c) and after Cd(II) (10mM) adsorption (d)-(i), showing the algae surface structure, with a wrinkled pattern of 10 - 20 microns (a) – (f), transversal section of the algae tallus showing cellulose fibers (g) – (i) and Cd(II) microcrepitates formed on algae surface (d) – (i). Scale is 100 microns for (a), (d) and (g), 10 microns for (b), (e) and (h) and 3 microns for (c), (f) and (i).

Given the size of the $CdCO_3$ precipitates, one can interpret that they resulted from the combined effect of sample preparation and drying under the electron beam; however, further investigations using synchrotron XRF spectroscopy under cryo-conditions confirmed that precipitation occurred as an influence of alkaline pH (see Figure **6** below).

Synchrotron XRF and XAS

XRF maps showing the distribution of Cd(II) on *Fucus v.* at pH values of 5, 7 and 9 are presented in **Figures 6b, c, d**. All the maps show the distribution of Cd(II) (red) onto the algae surface with respect to the resolution used for data collection, of 3 microns step size. The distribution has various degrees of heterogeneity and is most visible as hotspots at pH 9, indicating the formation of micro precipitates (**Figure 6d**). Spatial distribution correlations between Cd(II) (red) and other elements like Ca (blue) and

K (green) were observed and quantified at pH 5 and 7, which may be related with the exchange of lighter ions by Cd(II) at the algae surface (Brinza et al., 2019). We used XRF maps to guide the selection of several points of interest (POIs) for XANES analysis containing high, medium, and low concentrations of Cd(II).

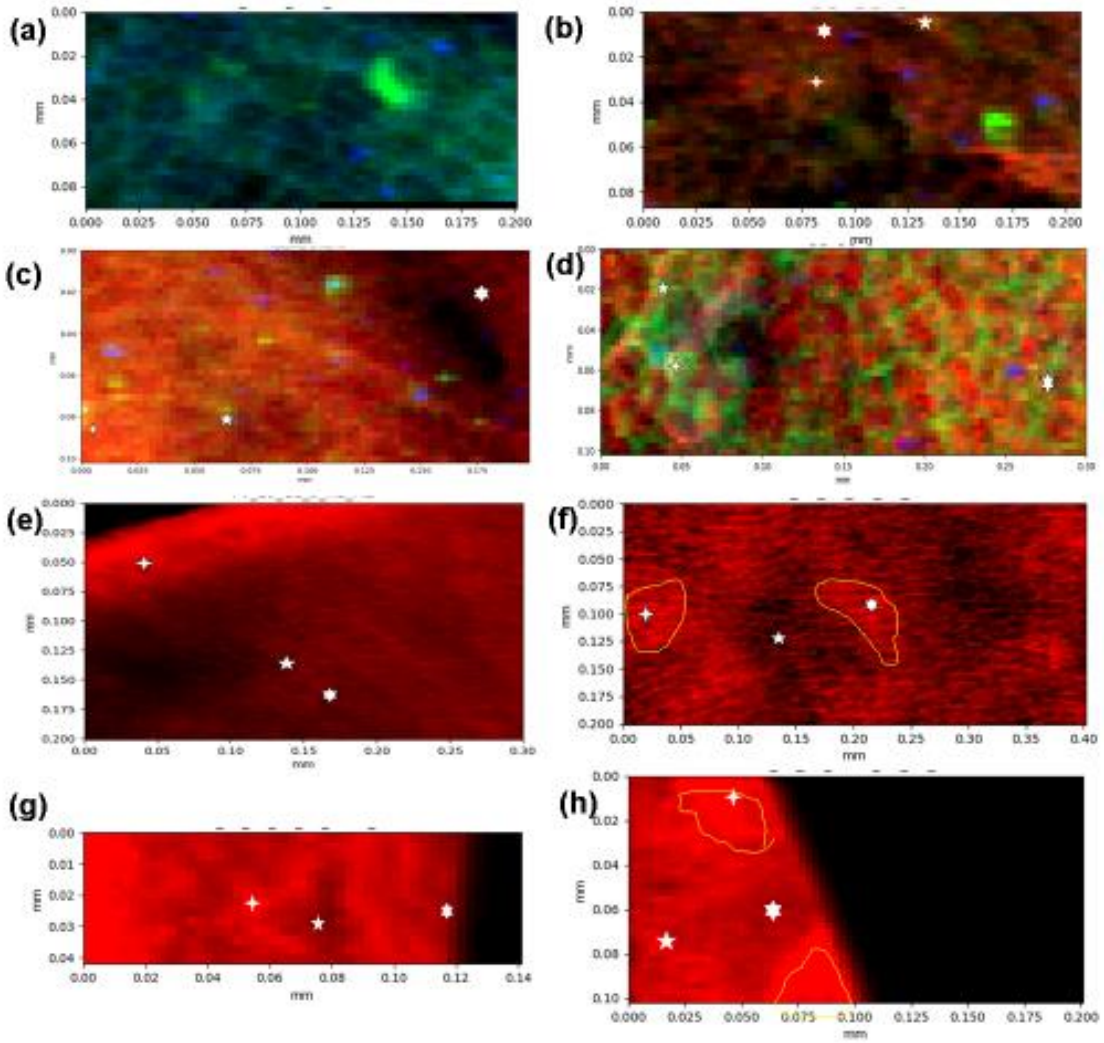

Figure 6. XRF elemental maps showing the microscale distribution of Cd(II) (red), K (green) and Ca (blue) onto the algae surface as collected from the sea (blank with no Cd, only K and Ca), **(a)** and after adsorption at: pH 5, $C_{Cd(II)}$ 1mM **(b)**, pH 7, $C_{Cd(II)}$ 1mM **(c),** pH 9, $C_{Cd(II)}$ 1mM **(d),** pH 5, $C_{Cd(II)}$ 10mM **(e)**, after the fourth cycle using 10 mM HCl, pH 5, $C_{Cd(II)}$ 10mM **(f),** after the third cycle using 10 mM NaOH, pH 5, $C_{Cd(II)}$ 10mM **(g),** and after the forth cycle using 1 mM EDTA, pH 5, C_{Cd} 10mM **(h)**. Marked on each map as white stars, from simple stars with 4 corners, stars with 5 corners to more complex ones with 6 corners, respectively, are the selected POIs, POI1, POI2 and POI3, at different Cd(II) concentrations, from which XANES spectra were collected. Step size resolution is 3 microns, and the map scale is in

millimetres. Acquisition time per point is 1.5 sec per point for map (**a, e, f, g, h**), and 0.5 sec per point for maps (**b, c, d**).

Figure 6b and e show the spatial distribution of Cd(II) onto *Fucus v.* at different concentrations. High concentration of Cd(II) in solution (10mM) led to a homogeneous distribution of Cd(II) adsorbed onto the algae surface indicating even adsorption and saturation of algae surface sites (**Figure 6e)**. This supports the kinetic profile presented in **Figure 1b**.

Figure 6b, c, d show the distribution of Cd(II) (red), Ca(blue) and K(green) on *Fucus v.* at pH values of 5, 7 and 9. Some areas on maps at pH 5 and 7 show coexistence of Cd, K and/or Ca indicating possible exchange of lighter ions with Cd(II) at the algae surface (Brinza et al., 2019).

Figure 6 also shows the spatial distribution of Cd(II) in repetitive sorption desorption cycles using HCl, NaOH and EDTA as eluents; after the first adsorption cycle (**Figure 6e**), after the fourth cycle using 10 mM HCl (**Figure 6f**)**,** after the third cycle using 10 mM NaOH (**Figure 6g**), and after the fourth cycle using 1mM EDTA (**Figure 6h**). All these maps show a heterogeneous spatial distribution of Cd(II) with localized concentrations in regions of ca. 50 microns (**Figures 6f, 6h**). This indicates that Cd(II) is still adsorbed in a substantial amount after algae reuse, even in some regions, Cd(II) concentrations have become richer likely forming agglomerates or microprecipitates. Cd XANES spectra collected at selected POIs at various Cd(II) concentrations from samples at pH 5, 7 and 9, and after desorption cycles using HCl, EDTA and NaOH are presented in **Figure 7**.

The fingerprint assessment and comparison of the Cd-L_3 Edge XANES show similarities among spectra collected from POIs and standards (Cd(II) in alginate and Cd(II) in CMC) with respect to general features such as: pre-edge at ca 3540.5eV, white line pre-shoulder at about 3550 eV, white line around 3566 eV, and first amplitude after the white line, of which its highest amplitude vary from 3610 to 3620 eV. However, the spectra are not identical among them and are different to spectra of pure Cd(II) organic standards indicating that Cd(II) speciation at the algae surface consists in a mixture of Cd(II) species bound onto functional groups of cellulose fibres and alginate, which are major constituents of the algae cell wall. Thus, XANES spectra of each representative POI collected from the samples were further analysed using LCF analysis (**Table 3**). **Tables SI 3 – 5** shows all the fits for each spectrum and the ones highlighted in bold are considered the best achieved in terms of R-factor and red χ^2.

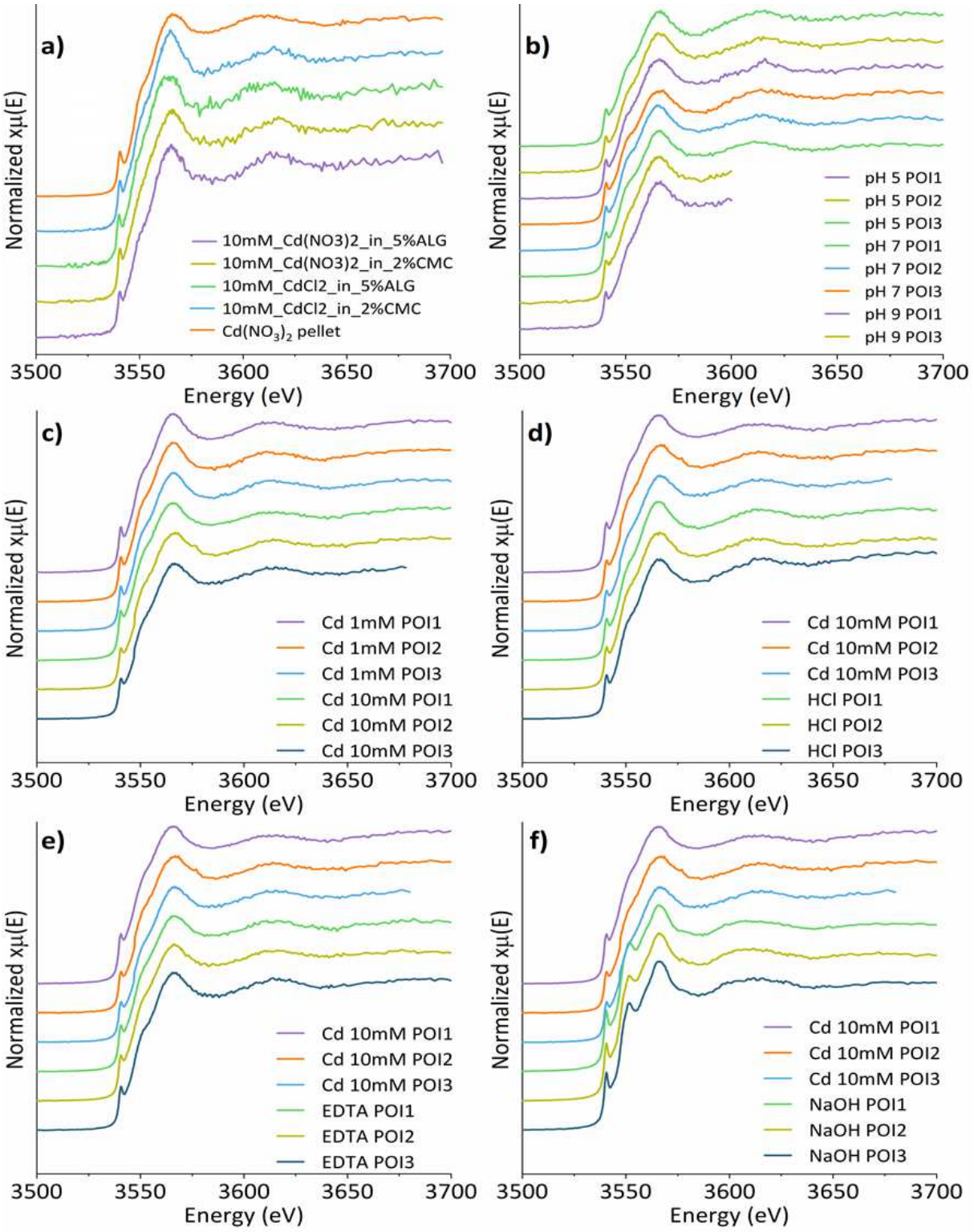

Figure 7. Cd(II) L3 adsorption edge XANES spectra of standards and the selected POIs marked on the XRF maps (Figure 5). POI1, POI2 and POI3, are marked on each map as white stars, from simple stars with 4 corners, stars with 5 corners to more complex ones with 6 corners, respectively. The last two POIs at pH 9, the XANES spectra were cut because there was a K absorption edge starting to appear and this would have led to Cd spectra alteration.

LFC results from samples at different pH values indicate a variety of Cd(II) species are bound onto the algae surface; $Cd(NO_3)_2$ in 2%CMC contributed significantly to the spectrum (33 to 60%), $Cd(NO_3)_2$ in 5%ALG (4-42%) and $CdCl_2$ in 2%CMC (26%) (**Table 3 and Table SI 3**). These results suggest that Cd(II) at pH 5, is mainly bound to carboxylic functional groups of cellulose fibres and alginate. As pH increases to 7, the LCF results show that Cd(II) species bound onto algae surface are the cellulose type, with a high proportion (67%) of Cd(II) as $CdCl_2$ in 2%CMC alike species and up to 52% as $Cd(NO_3)_2$ in 2%CMC alike species. This may suggest an increasing role of cellulose functional groups in Cd(II) uptake at neutral pH likely combined to enhanced activity of seawater chlorinated compounds. In contrast, a single type of species of Cd(II) bound to cellulose functional groups was identified at pH 9 as indicated by the fit to the $CdCl_2$ in 2%CMC standard.

Table 3. Summary table of Cd-L_3 edge XANES - Linear combination fittings (as best R and χ^2 of all combinations of normalized μ(E) from-20 to +150eV around the edge, namely 3527-3697 eV) results (weights sum forced to 1, weights not forced between 0 to 1, fitted E0, 240 data points and 5 variables)

POIs ID/ STD	$Cd(NO_3)_2$ in 5% ALG	$CdCl_2$ in 5% ALG	$Cd(NO_3)_2$ in 2% CMC	$CdCl_2$ in 2%CMC	$Cd(NO_3)_2$ pellet	R-factor	Reduced chi-square
pH 5 POI1	42.9±3.7	2.0±0.4	60.4±4.2	0*	9±0.8	0.00109	0.000148
pH 5 POI2	28.5 ±4.1	3.8±0.6	32.9±3.2	26.3±5.6	8.4±8.7*	0.00085	0.000118
pH 5 POI3	3.9±4.3	4.7±0.2	36.7±4.3	26.0±7.4	28.7±2.9	0.00132	0.000174
pH 7 POI1	NI	FE	52.3±5.5	47.7±5.8	NI	0.00413	0.000543
pH 7 POI2	9.5±0.8*	EF	23.0±4.9	67.6±4.7	NI	0.00184	0.000249
pH 7 POI3	43.6±6.8	0*	27.1±7.0	10.2±1.4	24.4±4.6	0.00353	0.000454
pH 9 POI1	FE	FE	0*	57.9±3.0	45.0±3.2	0.00109	0.00019
pH 9 POI3	0*	FE	FE	100±0	0*	0.00252	0.000406
Cd 1mM POI1	0*	3.0±6.7*	43.2±3.8	18.3±4.3	38.0±3.4	0.00071	0.000105
Cd 1mM POI2	NI	NI	54.1±3.5	25.5±3.3	20.4±5.5	0.00109	0.00015
Cd 1mM POI3	18.3±7.1	3.0±1.8*	52.4±5.0	21.0±4.0	5.3±0.9	0.00109	0.000156
Cd 10mM POI1	0*	7.5±2.2	83.8±6.4	8.5±0.7	0	0.00181	0.000239
Cd 10mM POI2	4.4±1.0*	1.8±1.7*	49.5±5.8	19.3±8.2	25.0±3.1	0.00193	0.000263
Cd 10mM POI3	0*	0*	37.3±3.0	0*	54.6±2.7	0.00093	0.00013
HCl POI1	15.7±2.8	0*	34.2±2.9	24.8±5.6	27.1±2.6	0.00048	0.000068
HCl POI2	FE	FE	59.7±4.7	14.5±3.5	25.8±2.4	0.00113	0.000155
HCl POI3	0.9±0.8*	0*	54.4±3.6	16.3±4.3	34.7±6.9	0.00089	0.000123
EDTA POI1	7.2±0.6	0*	61.5±6.0	0*	39.0±4.2	0.00138	0.000186
EDTA POI2	5.0±2.0*	4.8±1.8*	76.2±7.0	0*	42.7±4.2	0.00131	0.000176
EDTA POI3	NI	NI	56.4±5.8	12.9±3.5	30.7±2.2	0.00107	0.000148
NaOH POI1	Not processed, XANES spectra very much alike $CdCO_3$ [75], suggesting Cd(II) precipitation as otavite.						

NI=not included, FE=excluded by the fit* = compound not significant in this POIs as either the error was too large, or it has a negative weight which suggests that these are not in the sample POI.

549 The best fits with the 0* compared to and as opposed to the ones without the 0*species (labelled as NI)
550 indicate that the 0* are not in the mixture of the POI and suggests that potentially other species (to which
551 we lack the standard spectra for) are part of the mix.

552 A visual comparison of the spectra from the different POIs with different concentrations of Cd(II) (1 and
553 10 mM Cd(II), **Figure 7c**) show minor differences among the spectra. Spectra from the algae exposed
554 to the highest concentration of Cd(II) used (Cd_10mM; POI2 and POI3) showed distinctive features on
555 the pre-shoulder in the region of the white line (3540 – 3550 eV) that are not present in other POIs. A
556 similar feature is observable in the spectrum of the $Cd(NO_3)_2$ standard, potentially indicating that some
557 Cd(II) was adsorbed as $Cd(NO_3)_2$ onto the algae surface. Other features vary among the spectra, the
558 position and intensity of the white line as well as the intensity of first amplitude after the white line (3610
559 - 3620 eV). These minor differences were validated and quantified by LCF analysis in **Table 3 and**
560 **Table SI 4**.

561 A major difference in the fingerprint of the XANES spectra was observed when NaOH was used as
562 eluent (POIs 1-3**, Figure 7e**). The three spectra show a prominent feature between the pre-edge and
563 the white line at an energy of ca. 3556 eV. Unfortunately, none of our standards were alike these spectra,
564 but a similar spectrum has been reported for $CdCO_3$ (Siebers et al., 2012).

565 Spectra from algae samples after desorption using HCl and EDTA eluents showed minor differences
566 among them (**Figures 7d – f**), which were quantified by LCF and presented in **Table 3** and detailed in
567 **Table SI 5**. When HCl solution was used as eluent, Cd(II) species onto the algae surface did not change
568 significantly between the first and the fourth adsorption cycle. Thus, the majority of Cd(II) remained
569 adsorbed as Cd $(NO_3)_2$ onto CMC (HCl_POI2 - 59%), followed by up to a quarter of Cd(II) species been
570 alike $CdCl_2$ onto CMC (HCl_POI1 - up to 24%,) and the rest alike Cd $(NO_3)_2$ (HCl_POI3 - up to 34%).
571 These results suggest that 10mM HCl led to protonation of hydroxyl and carboxyl functional groups of
572 cellulose fibres playing an essential role in Cd(II) uptake. The presence of chloride ions led to a sensible
573 increase of $CdCl_2$ alike species bound onto algae surface. When EDTA was used as an eluent, a
574 substantial increase (from 56-76%) of Cd(II) species alike $Cd(NO_3)_2$ in 2% CMC, (EDTA_POIs 1-3 in
575 **Table 3 and Table SI 5**), with additional species alike $Cd(NO_3)_2$ pellets was derived from LCF analyses.
576 This indicates that Cd(II) has preponderantly bound onto cellulose functional groups potentially
577 complexing and additionally micro precipitating as nitrate.

578 LCF analysis for the spectra collected from the reused algae eluted with NaOH could not be carried out
579 due to the fact that the spectra looked very different from the ones above and from any organic and

580 inorganic standards scanned during the beam time, in addition to the lack of an appropriate
581 representative standard. Reported data of Cd L_3-absorption edge XANES are very limited in literature
582 and databases (Cibin et al., 2020; Ewels et al., 2016; Mathew et al., 2018); however, a $CdCO_3$ spectra
583 (Siebers et al., 2012) was found alike to the ones obtained from our algae samples eluted with NaOH
584 solution and reused. This led us to conclude that a relatively strong (concentrated) basic eluent, such
585 as 10 mM NaOH, used in repetitive cycles appeared to enhance Cd(II) precipitation, as $CdCO_3$ at the
586 algae surface. This agrees with solution chemistry simulation (**Figure 1)** and diffraction data confirmation
587 **(Figure SI 2**).

588 As Cd L_3 edge XAS data on algae biomass systems are not available in literature, a direct comparison
589 of our results is limited; however, to emphasise on the applicability of the new approach for atomic
590 investigation of the uptake mechanism, two studies found in the literature are briefly mentioned.
591 Comparing XAS results of other metals absorbed onto *Fucus v.*, we have previously shown in
592 experiments at low pH that Zn(II) is bound onto the Irish *Fucus v.* mainly by carboxylic groups from the
593 alginate components, such as guluronic and mannuronic residues in which Zn coordinates with 5 and 6
594 O atoms at distances of 1.98–2.03 Å (Brinza et al., 2019). Cd XAS results in comparison to those of Zn,
595 using the same bio sorbent (Brinza et al., 2019) confirms similarities of metals uptake mechanisms
596 regarding their binding to carboxyl and hydroxyl functional groups in alginate and cellulosic components
597 of the algae, to a certain extent. Interestingly, LCF indicate that at low pH, Cd, as compared to Zn, has
598 a greater affinity for cellulosic component of the Irish kelp cell wall and less for alginate. In addition,
599 current Cd XAS results showed evidence of Cd(II) microprecipitation as carbonates on the algae surface
600 at high pH when basic solution is used as eluent biomass reuse.

601 From the algae habitat point of view, Zn-XANES data has showed that Zn adsorbed onto the Baltic
602 *Fucus v.*, bounds predominantly to the cellulosic component of algae cell wall, as opposed to the alginate
603 one. The binding dependency to specific functional groups is a function of algae seasonal metabolism,
604 harvesting, and the Zn source (Brinza et al., 2020).

605 **FTIR results**

606 FTIR data of wet algae tissue before and after adsorption and desorption treatments are presented in
607 **Figure 8** and interpreted in the text aided by vibrations identification as in **Table SI 6**. Variable and broad
608 vibrations in the range of 3200-3600 cm^{-1} are assigned to –OH, hydroxyl intermolecular functional

groups (Andy, 2015; Jawad et al., 2020). This broad peak is present in all spectra of the algae species as well as alginate and cellulose standards. It is observable that the large peak of all algae with Cd(II) are shifted towards higher wavenumber suggesting their involvement to Cd(II) binding.

The large peak at 2893 cm^{-1} present in cellulose standard (**Figure 8 b**) indicative of C-H stretching is separated in two peaks (at varying wavenumber from about 2922 to 2852 cm^{-1}) in all algae spectra containing Cd(II) and lightly visible in spectra of the blank algae. This indicates that the C-H cellulose functional groups may also be involved in Cd(II) accommodation within cellulose fibres or binding, potentially via H bonding.

A shoulder at about 1730 cm^{-1} is observable in the algae spectra from multiple elution cycle experiments with HCl and EDTA. This feature can be assigned to acyl chloride (-COCl) functional groups (Brunning, 2015), which may have derived from reactive carboxylic acids that were chlorinated by HCl and/ during metal desorption by elution and algae functioning or seawater chloride traces that remained on algae surface.

Carboxyl (-COOH) functional groups are identified in the range of wavenumbers from 1670–1760 cm^{-1} for C =O groups and 1000–1300 cm^{-1} for C–O groups (Boenke, 1998; LibreTexts, 2019).FTIR signal at around 1620 cm^{-1} could be assigned to C=O stretching in carbonyl functional groups or/and double C=C stretching in alkenes. These vibrations which are most probable indicative of C=O functional groups from carboxyl of alginate and cellulose (as they are present in both standards, but slightly shifted and less intense) and are present in all *Fucus v.* species. They are very intense/strong in algae samples after interaction with Cd(II) solutions and less intense in blank *Fucus v.*; however, they are all slightly shifted (1632 - 1618 cm^{-1}), towards higher wavenumber as compared to the signal in the spectra of alginate standard and blank algae. This indicates that likely the C=O functional groups of alginate are involved in Cd(II) binding. It is noticeable that the vibration at around 1620 cm^{-1} is shifted coherently towards lower wavenumber as the pH decreases (surface protonates) and the Cd(II) concentration increases (more Cd(II) species are available), indicating that these functional groups play an important role in Cd(II) binding.

The broad peak with higher intensity at 1454 cm^{-1} in the blank spectra is indicative of in-plane bending of –OH (Michalak et al., 2018). The same vibration is present as a small shoulder in the spectra at pH 5 but absent in the rest of the spectra. Accounting on surface saturation with Cd at lower Cd(II)

concentration (see kinetic results, **Figure 2**) this may be indicating unoccupied hydroxyl groups at algae surface.

Broadened and shifted towards lower wavenumber peaks at 1420 cm^{-1}, 1419 cm^{-1} and 1415 cm^{-1} for samples at pH 5, 7 and 9 respectively, might be associated with symmetric bending of CH_2 and/or symmetric stretching of CO_3 (Coates, 2006; Michalak et al., 2018). In agreement with our XRD and solution chemistry simulation results, these vibrations, which shifted coherently toward lower wavenumber as pH increases, indicate the presence of carbonates ions in higher concentration as the pH increases. These vibrations appear very intense in the spectra of the algae eluted with HCl and EDTA, indicating the presence of CH_2 and carbonates ions in the system and at algae surface post adsorption, respectively, that were unveiled by washing the existent algae carboxyl and by supplementing them on algae surface by complexation with COOH and CH_2 from EDTA. The quantitative increase of these functional groups for the HCl and EDTA systems supports the higher quantitative uptake of Cd in subsequent cycles as shown in Figure 4 and described in appropriate section above. Interestingly, this vibration is very broad and has its high intensity extended to 1376 $cm^{-1}$for the spectra of *Fucus v.* reused in multiple adsorption cycles and eluted with NaOH, which could be related to the overlap of an C-H compounds as they are characterised by vibrations at 1373 cm^{-1} (Michalak et al., 2018).

Double vibration with the highest intensity of the peaks at 1190 cm^{-1} and 1300 cm^{-1} are observable in the spectra of all algae species. They can be associated with various functional groups like C-O stretching in carboxyl functional groups, wagging vibrations of C-H (Andy, 2015), bending vibrations of C-H and O-H, rocking vibrations of CH_2 in polysaccharide or tertiary amine bands (Michalak et al., 2018).

Finally, vibrations between 1200 cm^{-1} and 900 cm^{-1} are also present in all the spectra, which we can be assigned to stretching vibrations of C-O-C and C-C, rocking vibrations of CH_2, stretching vibrations of carbonate (CO_3^{2-}) and mono-protonated (HCO_3^-) carbonates ions as well as bending vibrations of a ring, possibly from cellulose structure (Michalak et al., 2018).

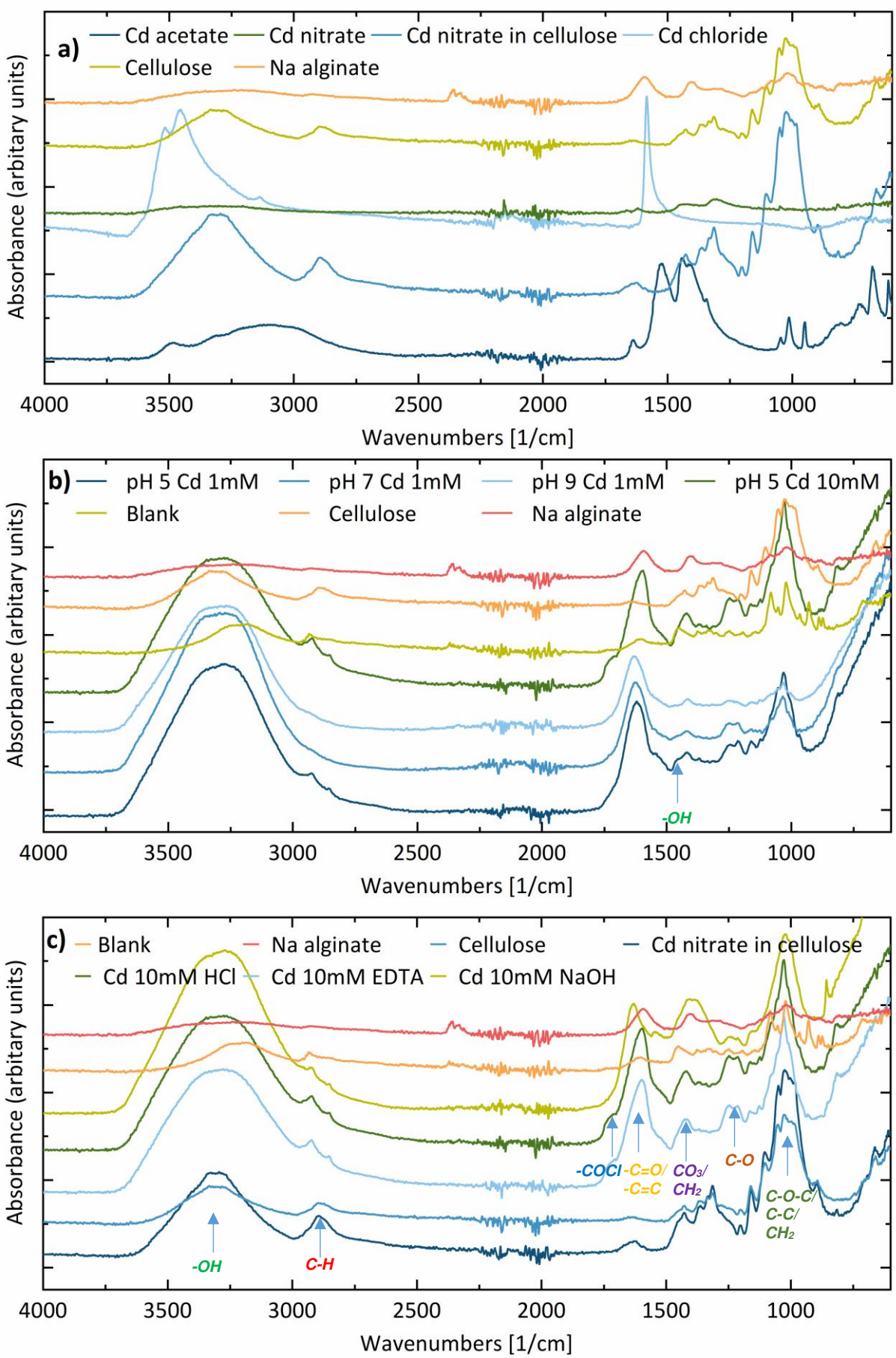
a)
Cd acetate
Cd nitrate
Cd nitrate in cellulose
Cd chloride
Cellulose
Na alginate
Absorbance (arbitary units)
4000
3500
3000
2500
2000
1500
1000
Wavenumbers [1/cm]
b)
pH 5 Cd 1mM
pH 7 Cd 1mM
pH 9 Cd 1mM
pH 5 Cd 10mM
Blank
Cellulose
Na alginate
-OH
Absorbance (arbitary units)
Wavenumbers [1/cm]
c)
Blank
Na alginate
Cellulose
Cd nitrate in cellulose
Cd 10mM HCl
Cd 10mM EDTA
Cd 10mM NaOH
-COCl
-C=O/
-C=C
CO3/
CH2
C-O
C-O-C/
C-C/
CH2
-OH
C-H
Absorbance (arbitary units)
Wavenumbers [1/cm]

664

665

666 **Figure 8**. FTIR spectra of algae after adsorption at (a) various pH values, (b) various Cd(II)
667 concentration, and (c) various type of eluents used.

668 Overall, our FTIR results suggests that functional groups involved in Cd bonding are C-O or
669 C=O or COCl from carboxyl (-COOH) as well as hydroxyl (-OH) groups of alginate and cellulosic
670 components, in various degree of substitutions. C-H and CH_2 play and important role in Cd binding and
671 carbonate (CO_3^{2-}) and mono-protonated (HCO_3^-) proves the formation of otavite. In addition, sulphur
672 and phosphorus groups, amino and nitro groups as well as carbonyl and methyl and methylene groups
673 were identified on the algae surface in agreement with reported data (He and Chen, 2014).

674 Comparing our FTIR results with the literature findings, a good agreement could be seen
675 and additionally, the current results show evidence of carbonate functional groups been involved in
676 Cd(II) uptake by carbonate formation and microprecipitation (Abbas et al., 2014; Ahmady-Asbchin
677 and Jafari, 2013; Brinza et al., 2019; He and Chen, 2014; Henriques et al., 2017; Kanchana et al.,
678 2014; Lodeiro et al., 2005; Mata et al., 2009; Mazur et al., 2018; Zeraatkar et al., 2016).
679 In relation to the above computing and experimental approaches (i.e., geochemical modelling, XRD,
680 and XAS), the FTIR results supports that Cd(II) coordinates to the oxygen atoms of hydroxyl groups,
681 carboxyl groups, pyranose cycle and carbonate, forming weak bonding such as H bonds, strong
682 chemical bonding via substitution or complexation and microprecipitation.

683 From a mechanistic point of view, generally, our studies so far on the Irish kelp showed that Zn
684 and Cd uptake occurs via ion exchange, chemical and physical adsorption mechanisms, involving
685 covalent and hydrogen bonds respectively. Main functional groups that are involved in metals binding
686 are carboxyl and hydroxyl – function of solution pH. Additionally, the new approach of using synchrotron
687 investigations, beside FTIR, showed that Zn has preferential affinity for carboxyl functional groups from
688 alginate component of the cell wall, while Cd binds preferentially, but not exclusively, on carboxyl
689 functional groups of cellulosic components. The results also suggested that the mechanisms of metals
690 uptake as well as quantitative assessment vary as a function of metals type, biomass specie, cell wall
691 components and their habitat, as well as process conditions, fact that encourages further test of other
692 metals on the chosen Irish kelp, as bio sorbent, before its testing on real effluents and further process
693 optimization and scaling up.

694

Conclusions

Our comprehensive qualitative and quantitative investigations of Cd(II) speciation in solution and at algae surface, took the usually laboratory based investigations to a next level by employing highest resolution synchrotron micro XRF and XAS techniques, as a least common approach and chemically nondestructive analytical techniques, to provide direct information about biosorption mechanism.

Quantitatively wise, the surface of the Irish brown algae (*Fucus v.*) is a very good sorbent for Cd(II) species (max uptake capacity of 1.203 mmol g^{-1}). Cd adsorption initiates rapidly (~2 h) before reaching a steady stage over a range of pH between 5 and 7. Based on our kinetic modelling, the adsorption predominantly occurs as a physical mechanism involving weak interactions (i.e., hydrogen bonds or Van der Walls forces), followed by the formation of stronger chemical bonds (chemisorption) and at high pH (>9) - micro precipitation. FTIR results and linear combination fitting (LCF) of XANES spectra demonstrate that Cd(II) adsorbed by the Irish kelp occurs in various chemical forms depending on the type of eluent used. The most common species at low pH (5) are Cd(II) bound to carboxylic functional groups of cellulose fibers (26 to 60%) and Cd(II) bound to alginate (4-42%). At pH 7, Cd(II) is preponderantly bound to cellulose.

The use of HCl at low concentration (10 mM) allows Cd desorption and the restoration of weak binding forces; however, this process can only be performed up to 3 cycles before the algae tissue become affected. The use of EDTA (1mM) activates the surface for stronger chemical interaction providing good results for metal elution and algae reuse in 2-3 cycles. The results suggest that the use of less concentrated solution of HCl and EDTA may lead to algae reuse in more than 3 cycles, avoiding algae tissue damage. Interestingly, the use of HCl and EDTA eluents for metals recovery and bio sorbent functioning led to significative increase of Cd uptake (quantitatively more than double) as compared to the first cycle. This increase was due to eluents effect on surface sites, namely: (a) HCl most probably desorbed not only Cd but also other ions, freeing and/or protonating new binding sites for more Cd to be adsorbed in subsequent cycles and (b) EDTA desorbed Cd and potentially other ions, by complexation, and functioned new active surface sites for more Cd to bind in subsequent cycles. The use of NaOH (10 mM) impacted negatively the performance of the brown algae as an adsorbent for Cd(II) being effective only for the first cycle and promoting Cd(II) micro precipitation after multiple uses.

Overall, *Fucus v.* is an excellent bio sorbent to immobilize and remove Cd(II) from aqueous media, with applications to the current water treatments, through future optimization and scaling up to an algal based biotechnology. We suggest that further studies must be performed in pilot experiments to test the bio sorbent in fixed-bed and fluidized-bed column reactors using real Cd(II) polluted effluents. Also, the results have significant implications on our understanding of the uptake of Cd(II) onto algal biomass under the context of algae potential to become a green bio adsorbent in clean, environmental eco-friendly biotechnologies – concept and strategy in assistance of environmental sustainability. In addition, these outputs might be transposed to the context of marine algae - as a potential food supply.

Acknowledgements

We acknowledge Diamond Light Source (DLS), UK for beam time on Beamline I18 under Proposal SP24321-1. XAS data modelling is a part of a project that has received partial funding from the Romanian Ministry of Research and Innovation within Program 1 - Development of the national RD system, Subprogram 1.2 - Instructional Performance – RDI excellence funding projects (Contract no. 34PFE). Adsorption experiments and their kinetic modelling, geochemical modelling, Cd(II) analyses and XRD work were carried out at the Alexandru Ioan Cuza University of Iasi, Romania. The ATR-FTIR spectroscopy data were collected, at the DLS, beamlines I18 and B23. SEM work was carried out at the University of Leeds, UK. The authors declare no competing financial interest.

References

Abbas, S.H., Ismail, I.M., Mostafa, T.M., Sulaymon, A.H., 2014. Biosorption of Heavy Metals: A Review. Journal of Chemical Science and Technology 3(4), 74-102.

Ahmady-Asbchin, S., Andrès, Y., Gérente, C., Cloirec, P.L., 2008. Biosorption of Cu(II) from aqueous solution by Fucus serratus: Surface characterization and sorption mechanisms. Bioresource Technology 99(14), 6150-6155.

Ahmady-Asbchin, S., Jafari, N., 2013. Cadmium biosorption from aqueous solutions by fucus vesiculosus L.: Sorption Mechanisms. International Journal on Algae 15(1), 91-102.

Ahmed, M.B., Zhou, J.L., Ngo, H.H., Guo, W., Thomaidis, N.S., Xu, J., 2017. Progress in the biological and chemical treatment technologies for emerging contaminant removal from wastewater: A critical review. Journal of Hazardous Materials 323, 274-298.

Al-Ghouti, M.A., Da'ana, D.A., 2020. Guidelines for the use and interpretation of adsorption isotherm models: A review. Journal of Hazardous Materials 393, 22.

Anastopoulos, I., Kyzas, G.Z., 2015. Progress in batch biosorption of heavy metals onto algae. Journal of Molecular Liquids 209(Supplement C), 77-86.

Andy, B., 2015. Compound Interests. https://www.compoundchem.com/2015/02/05/irspectroscopy/. (Accessed 11th February 2020 2020).

Arumugam, N., Chelliapan, S., Kamyab, H., Thirugnana, S., Othman, N., Nasri, N.S., 2018. Treatment of Wastewater Using Seaweed: A Review. Int J Environ Res Public Health 15(12).
Ayawei, N., Ebelegi, A.N., Wankasi, D., 2017. Modelling and Interpretation of Adsorption Isotherms. Journal of Chemistry 2017, 3039817.
Azari, A., Gholami, M., Torkshavand, Z., Yari, A., Ahmadi, E., Kakavandi, B., 2015. Evaluation of basic violet 16 adsorption from aqueous solution by magnetic zero valent iron-activated carbon nanocomposite using response surface method: Isotherm and kinetic studies. Journal of Mazandaran University of Medical Sciences 25, 333-347.
Azari, A., Nabizadeh, R., Nasseri, S., Mahvi, A.H., Mesdaghinia, A.R., 2020. Comprehensive systematic review and meta-analysis of dyes adsorption by carbon-based adsorbent materials: Classification and analysis of last decade studies. Chemosphere 250, 126238.
Azari, A., Noorisepehr, M., Dehghanifard, E., Karimyan, K., Hashemi, S.Y., Kalhori, E.M., Norouzi, R., Agarwal, S., Gupta, V.K., 2019. Experimental design, modeling and mechanism of cationic dyes biosorption on to magnetic chitosan-lutaraldehyde composite. International Journal of Biological Macromolecules 131, 633-645.
Azari, A., Salari, M., Dehghani, M.H., Alimohammadi, M., Ghaffari, H., Sharafi, K., Shariatifar, N., Baziar, M., 2017. Efficiency of magnitized graphene oxide nanoparticles in removal of 2,4-dichlorophenol from aqueous solution. 26, 265-281.
Bdour, A.N., Hamdi, M.R., Tarawneh, Z., 2009. Perspectives on sustainable wastewater treatment technologies and reuse options in the urban areas of the Mediterranean region. Desalination 237(1), 162-174.
Bethke, C.M., 2002. The Geochemist`s Workbench - A User`s Guide to Rxn, Act2, React, and Gtplot, Release 4.0 ed., University of Illinois.
Boenke, A., 1998. The Standards, Measurements and Testing Programme (SMT) - the European support to standardisation, measurements and testing projects and its proposed activities in the 5th Framework Programme. Journal of near Infrared Spectroscopy, Vol 6 1998, A1-A6.
Brinza, L., Dring, M.J., Gavrilescu, M., 2005. Ability of different algal species to uptake heavy metals from wastewater, 68 ed. British Phycological Society, p. 30.
Brinza, L., Dring, M.J., Gavrilescu, M., 2007. Marine micro and macro algal species as biosorbents for heavy metals. Environmental Engineering and Management Journal 6, 237-251.
Brinza, L., Geraki, K., Breaban, I.G., Neamtu, M., 2019. Zn adsorption onto Irish Fucus vesiculosus: Biosorbent uptake capacity and atomistic mechanism insights. Journal of Hazardous Materials 365, 252-260.
Brinza, L., Geraki, K., Cojocaru, C., Holdt, S.L., Neamtu, M., 2020. Baltic Fucus vesiculosus as potential bio-sorbent for Zn removal: Mechanism insight. Chemosphere 238, 124652.
Brinza, L., Nygård, C.A., Dring, M.J., Gavrilescu, M., Benning, L.G., 2009. Cadmium tolerance and adsorption by the marine brown alga Fucus vesiculosus from the Irish Sea and the Bothnian Sea. Bioresource technology 100(5), 1727-1733.
Brinza, L., Schofield, P.F., Hodson, M.E., Weller, S., Ignatyev, K., Geraki, K., Quinn, P.D., Mosselmans, J.F.W., 2014. Combining microXANES and microXRD mapping to analyse the heterogeneity in calcium carbonate granules excreted by the earthworm Lumbricus terrestris. Journal of Synchrotron Radiation 21(1), 235-241.
Brunning, A., 2015. Compound Interests. https://www.compoundchem.com/2015/02/05/irspectroscopy/. (Accessed 11th February 2020 2020).
Bwapwa, J.K., Jaiyeola, A.T., Chetty, R., 2017. Bioremediation of acid mine drainage using algae strains: A review. South African Journal of Chemical Engineering 24, 62-70.
Cardoso, S.L., Costa, C.S.D., Nishikawa, E., da Silva, M.G.C., Vieira, M.G.A., 2017. Biosorption of toxic metals using the alginate extraction residue from the brown algae Sargassum filipendula as a natural ion-exchanger. Journal of Cleaner Production 165, 491-499.

Cardoso, S.L., Moino, B.P., Costa, C., Silva, M., Vieira, M., 2016. Evaluation of metal affinity of Ag+, Cd2+, Cr3+, Cu2+, Ni2+, Zn2+ and Pb2+ in residue of double alginate extraction from Sargassum filipendula seaweed. Chemical Engineering Transactions 52, 1027-1032.
Castro, L., Blazquez, M.L., Gonzalez, F., Munoz, J.A., Ballester, A., 2017. Biosorption of Zn(II) from industrial effluents using sugar beet pulp and F-vesiculosus: From laboratory tests to a pilot approach. Science of the Total Environment 598, 856-866.
Cibin, G., Gianolio, D., Parry, S.A., Schoonjans, T., Moore, O., Draper, R., Miller, L.A., Thoma, A., Doswell, C.L., Graham, A., 2020. An open access, integrated XAS data repository at Diamond Light Source. Radiation Physics and Chemistry 175, 108479.
Coates, J., 2006. Interpretation of Infrared Spectra, A Practical Approach. Encyclopedia of Analytical Chemistry.
D'Amato, D., Droste, N., Allen, B., Kettunen, M., Lähtinen, K., Korhonen, J., Leskinen, P., Matthies, B.D., Toppinen, A., 2017. Green, circular, bio economy: A comparative analysis of sustainability avenues. Journal of Cleaner Production 168, 716-734.
Davis, T.A., Volesky, B., Mucci, A., 2003. A review of the biochemistry of heavy metal biosorption by brown algae. Water Research 37, 4311-4330.
Diaz-Moreno, S., Amboage, M., Boada-Romero, R., Brinza, L., Cibin, G., Dent, A., Freeman, A., Geraki, T., Hayama, S., Mosselmans, F., 2012. XRay Absorption Spectroscopy at Diamond Light Source: Three Complementary Beamlines to Deliver a Comprehensive Service. XAS Research Review(3).
Ewels, P., Sikora, T., Serin, V., Ewels, C.P., Lajaunie, L., 2016. A Complete Overhaul of the Electron Energy-Loss Spectroscopy and X-Ray Absorption Spectroscopy Database: eelsdb.eu. Microscopy and Microanalysis 22(3), 717-724.
Fang, D., Zhuang, X., Huang, L., Zhang, Q., Shen, Q., Jiang, L., Xu, X., Ji, F., 2020. Developing the new kinetics model based on the adsorption process: From fitting to comparison and prediction. Science of The Total Environment 725, 138490.
Fang, L.C., Zhou, C., Cai, P., Chen, W.L., Rong, X.M., Dai, K., Liang, W., Gu, J.D., Huang, Q.Y., 2011. Binding characteristics of copper and cadmium by cyanobacterium Spirulina platensis. Journal of Hazardous Materials 190(1-3), 810-815.
Fernandez, P.M., Vinarta, S.C., Bernal, A.R., Cruz, E.L., Figueroa, L.I.C., 2018. Bioremediation strategies for chromium removal: Current research, scale-up approach and future perspectives. Chemosphere 208, 139-148.
Gavrilescu, M., 2004. Removal of heavy metal from environment by biosorption. Engineering Life Science 4(3), 219-232.
Gavrilescu, M., Chisti, Y., 2005. Biotechnology - a sustainable alternative for chemical industry. Biotechnology Advances 23, 471-499.
González, A.G., Jimenez-Villacorta, F., Beike, A.K., Reski, R., Adamo, P., Pokrovsky, O.S., 2016. Chemical and structural characterization of copper adsorbed on mosses (Bryophyta). Journal of Hazardous Materials 308, 343-354.
Hannachi, Y., Hafidh, A., 2020. Biosorption potential of Sargassum muticum algal biomass for methylene blue and lead removal from aqueous medium. International Journal of Environmental Science and Technology.
Hayat, K., Menhas, S., Bundschuh, J., Chaudhary, H.J., 2017. Microbial biotechnology as an emerging industrial wastewater treatment process for arsenic mitigation: A critical review. Journal of Cleaner Production 151, 427-438.
He, J.S., Chen, J.P., 2014. A comprehensive review on biosorption of heavy metals by algal biomass: Materials, performances, chemistry, and modeling simulation tools. Bioresource Technology 160, 67-78.
Henriques, B., Lopes, C.B., Figueira, P., Rocha, L.S., Duarte, A.C., Vale, C., Pardal, M.A., Pereira, E., 2017. Bioaccumulation of Hg, Cd and Pb by Fucus vesiculosus in single and multi-metal contamination scenarios and its effect on growth rate. Chemosphere 171, 208-222.

Herrero, R., Cordero, B., Lodeiro, P., Rey-Castro, C., Sastre de Vicente, M.E., 2006. Interactions of cadmium(II) and protons with dead biomass of marine algae Fucus sp. Marine Chemistry 99(1), 106-116.
Ho, Y.-S., 2006. Review of second-order models for adsorption systems. Journal of Hazardous Materials 136(3), 681-689.
Ho, Y.S., McKay, G., 1998. A Comparison of Chemisorption Kinetic Models Applied to Pollutant Removal on Various Sorbents. Process Safety and Environmental Protection 76(4), 332-340.
Hubbe, M.A., Azizian, S., Douven, S., 2019. Implications of Apparent Pseudo-Second-Order Adsorption Kinetics onto Cellulosic Materials: A Review. BioResources; Vol 14, No 3 (2019).
Huguet, S., Bert, V., Laboudigue, A., Barthès, V., Isaure, M.-P., Llorens, I., Schat, H., Sarret, G., 2012. Cd speciation and localization in the hyperaccumulator Arabidopsis halleri. Environmental and Experimental Botany 82, 54-65.
Işıldar, A., van Hullebusch, E.D., Lenz, M., Du Laing, G., Marra, A., Cesaro, A., Panda, S., Akcil, A., Kucuker, M.A., Kuchta, K., 2019. Biotechnological strategies for the recovery of valuable and critical raw materials from waste electrical and electronic equipment (WEEE) – A review. Journal of Hazardous Materials 362, 467-481.
Jawad, A.H., Mohammed, I.A., Abdulhameed, A.S., 2020. Tuning of Fly Ash Loading into Chitosan-Ethylene Glycol Diglycidyl Ether Composite for Enhanced Removal of Reactive Red 120 Dye: Optimization Using the Box–Behnken Design. Journal of Polymers and the Environment 28(10), 2720-2733.
Jayakumar, R., Rajasimman, M., Karthikeyan, C., 2015. Optimization, equilibrium, kinetic, thermodynamic and desorption studies on the sorption of Cu(II) from an aqueous solution using marine green algae: Halimeda gracilis. Ecotoxicology and Environmental Safety 121, 199-210.
Kanchana, S., Jeyanthi, J., Kathiravan, R., Suganya, K., 2014. Biosorption of heavy metals using algae: a review. Int. J. Pharma Bio Sci. 3.
Kapahi, M., Sachdeva, S., 2019. Bioremediation Options for Heavy Metal Pollution. J Health Pollut 9(24), 191203.
Kaparapu, J., Prasad, M.K., 2018. Equilibrium, kinetics and thermodynamic studies of cadmium(II) biosorption on Nannochloropsis oculata. Applied Water Science 8(6), 9.
Kizilkaya, B., Dogan, F., Akgul, R., Turker, G., 2012a. Biosorption of Co(II), Cr(III), Cd(II), and Pb(II) Ions from Aqueous Solution Using Nonliving Neochloris Pseudoalveolaris Deason & Bold: Equilibrium, Thermodynamic, and Kinetic Study. Journal of Dispersion Science and Technology 33(7), 1055-1065.
Kizilkaya, B., Turker, G., Akgul, R., Dogan, F., 2012b. Comparative Study of Biosorption of Heavy Metals Using Living Green Algae Scenedesmus quadricauda and Neochloris pseudoalveolaris: Equilibrium and Kinetics. Journal of Dispersion Science and Technology 33(1-3), 410-419.
Kumar, D., Pandey, L.K., Gaur, J.P., 2016. Metal sorption by algal biomass: From batch to continuous system. Algal Research 18(Supplement C), 95-109.
Kumar Yadav, K., Gupta, N., Kumar, A., Reece, L.M., Singh, N., Rezania, S., Ahmad Khan, S., 2018. Mechanistic understanding and holistic approach of phytoremediation: A review on application and future prospects. Ecological Engineering 120, 274-298.
Lagergren, S., 1886. Zur theorie der sogenannten adsorption gelöster stoffe, K*ungliga Svenska Vetenskapsakademiens*. *Handlingar* 24(4), 1-39.
Langmuir, I., 1916. The constitution and fundamental properties of solids and liquids. Journal of American Chemical Society 38, 2221-2295.
LibreTexts, 2019. Infrared_Spectroscopy_Absorption_Table. https://chem.libretexts.org/Bookshelves/Ancillary_Materials/Reference/Reference_Tables/Spectroscopic_Parameters/Infrared_Spectroscopy_Absorption_Table. (Accessed 17/02/2020 2020).
Lodeiro, P., Cordero, B., Barriada, J.L., Herrero, R., Sastre de Vicente, M.E., 2005. Biosorption of cadmium by biomass of brown marine macroalgae. Bioresource Technology 96(16), 1796-1803.
Luna, A.S., Costa, A.L.H., da Costa, A.C.A., Henriques, C.A., 2010. Competitive biosorption of cadmium(II) and zinc(II) ions from binary systems by Sargassum filipendula. Bioresource Technology 101(14), 5104-5111.

Manceau, A., Bustamante, P., Haouz, A., Bourdineaud, J.P., Gonzalez-Rey, M., Lemouchi, C., Gautier-Luneau, I., Geertsen, V., Barruet, E., Rovezzi, M., Glatzel, P., Pin, S., 2019. Mercury(II) Binding to Metallothionein in Mytilus edulis revealed by High Energy-Resolution XANES Spectroscopy. Chemistry – A European Journal 25(4), 997-1009.
Mari, S., Huguet, S., Meyer, C.-L., Castillo-Michel, H., Testemale, D., Vantelon, D., Saumitou-Laprade, P., Verbruggen, N., Sarret, G., 2015. Evidence of various mechanisms of Cd sequestration in the hyperaccumulator Arabidopsis halleri, the non-accumulator Arabidopsis lyrata, and their progenies by combined synchrotron-based techniques Downloaded from. Journal of Experimental Botany 66.
Mata, Y.N., Blázquez, M.L., Ballester, A., González, F., Munoz, J.A., 2009. Biosorption of cadmium, lead and copper with calcium alginate xerogels and immobilized Fucus vesiculosus. Journal of Hazardous Materials 163, 555-562.
Mata, Y.N., Blázquez, M.L., Ballester, A., González, F., Muñoz, J.A., 2008. Characterization of the biosorption of cadmium, lead and copper with the brown alga Fucus vesiculosus. Journal of Hazardous Materials 158(2), 316-323.
Mathew, K., Zheng, C., Winston, D., Chen, C., Dozier, A., Rehr, J.J., Ong, S.P., Persson, K.A., 2018. High-throughput computational X-ray absorption spectroscopy. Scientific Data 5(1), 180151.
Mazur, L.P., Cechinel, M.A.P., de Souza, S.M.A.G.U., Boaventura, R.A.R., Vilar, V.J.P., 2018. Brown marine macroalgae as natural cation exchangers for toxic metal removal from industrial wastewaters: A review. Journal of Environmental Management 223, 215-253.
Mazur, L.P., Pozdniakova, T.A., Mayer, D.A., de Souza, S., Boaventura, R.A.R., Vilar, V.J.P., 2017. Cation exchange prediction model for copper binding onto raw brown marine macro-algae Ascophyllum nodosum: Batch and fixed-bed studies. Chemical Engineering Journal 316, 255-276.
Michalak, I., Mironiuk, M., Marycz, K., 2018. A comprehensive analysis of biosorption of metal ions by macroalgae using ICP-OES, SEM-EDX and FTIR techniques. Plos One 13(10), 20.
Moreira, V.R., Lebron, Y.A.R., Lange, L.C., Santos, L.V.S., 2019. Simultaneous biosorption of Cd(II), Ni(II) and Pb(II) onto a brown macroalgae Fucus vesiculosus: Mono- and multi-component isotherms, kinetics and thermodynamics. Journal of Environmental Management 251, 109587.
Nasab, S.M.H., Naji, A., Yousefzadi, M., 2017. Kinetic and equilibrium studies on biosorption of cadmium(II) from aqueous solution by Gracilaria corticata and agar extraction algal waste. Journal of Applied Phycology 29(4), 2107-2116.
Nie, Z.-y., Liu, H.-c., Xia, J.-l., Yang, Y., Zhen, X.-j., Zhang, L.-j., Qiu, G.-z., 2016. Evidence of cell surface iron speciation of acidophilic iron-oxidizing microorganisms in indirect bioleaching process. Biometals 29(1), 25-37.
OriginLab, 2007. Origin Pro, 8 ed., Northampton, USA.
Pyrzynska, K., 2019. Removal of cadmium from wastewaters with low-cost adsorbents. Journal of Environmental Chemical Engineering 7(1), 102795.
Qiu, H., Lv, L., Pan, B.-c., Zhang, Q.-j., Zhang, W.-m., Zhang, Q.-x., 2009. Critical review in adsorption kinetic models. Journal of Zhejiang University-SCIENCE A 10(5), 716-724.
Raftowicz-Filipkiewicz, M., 2016. The role of the circular economy in the implementation of the concept of sustainable development. Knowledge for Market Use 2016: Our Interconnected and Divided World, 400-404.
Ravel, B., Newville, M.A., 2005. ATHENA, ARTEMIS, HEPHAESTUS: data analysis for X-ray absorption spectroscopy using IFEFFIT. Journal of Synchrotron Radiation 12, 537-541.
Rodriguez-Couto, S., Shah, M., Biswas, J., 2021. Development in Wastewater Treatment Research and Processes: Removal of Emerging Contaminants from Wastewater through Bio-nanotechnology.
Romera, E., González, F., Ballester, A., Blázquez, M.L., Muñoz, J.A., 2007. Comparative study of biosorption of heavy metals using different types of algae. Bioresource Technology 98(17), 3344-3353.
Santibanez Gonzalez, E.D.R., Koh, L., Leung, J., 2019. Towards a circular economy production system: trends and challenges for operations management. International Journal of Production Research 57(23), 7209-7218.

961 Sari, A., Tuzen, M., 2008. Biosorption of cadmium(II) from aqueous solution by red algae (Ceramium
962 virgatum): Equilibrium, kinetic and thermodynamic studies. Journal of Hazardous Materials 157(2-3),
963 448-454.
964 Saxena, G., Kumar, V., Shah, M.P., 2020. Bioremediation for environmental sustainability : toxicity,
965 mechanisms of contaminants degradation, detoxification and challenges. Elsevier, Amsterdam.
966 Schlosser, D., 2020. Biotechnologies for Water Treatment, in: Filip, J., Cajthaml, T., Najmanová, P.,
967 Černík, M., Zbořil, R. (Eds.), Advanced Nano-Bio Technologies for Water and Soil Treatment. Springer
968 International Publishing, Cham, pp. 335-343.
969 Shah, M.P., Rodriguez-Couto, S., Kumar, V., 2021. New trends in removal of heavy metals from
970 industrial wastewater. Elsevier, Amsterdam.
971 Sheng, P.X., Ting, Y.P., Chen, J.P., Hong, L., 2004. Sorption of lead, copper, cadmium, zinc, and nickel
972 by marine algal biomass: Characterization of biosorptive capacity and investigation of mechanisms.
973 Journal of Colloid and Interface Science 275(1), 131-141.
974 Siebers, N., Kruse, J., Eckhardt, K.-U., Hu, Y., Leinweber, P., 2012. Solid-phase cadmium speciation in
975 soil using L-3-edge XANES spectroscopy with partial least-squares regression. Journal of synchrotron
976 radiation 19, 579-585.
977 Simonin, J.-P., 2016. On the comparison of pseudo-first order and pseudo-second order rate laws in
978 the modeling of adsorption kinetics. Chemical Engineering Journal 300, 254-263.
979 Sweetly, D.J., 2014. Macroalgae as a Potentially Low-Cost Biosorbent for Heavy Metal Removal: A
980 Review. International Journal of Pharmaceutical & Biological Archives 5(2), 17-26.
981 Vafajoo, L., Cheraghi, R., Dabbagh, R., McKay, G., 2018. Removal of cobalt (II) ions from aqueous
982 solutions utilizing the pre-treated 2-Hypnea Valentiae algae: Equilibrium, thermodynamic, and
983 dynamic studies. Chemical Engineering Journal 331(Supplement C), 39-47.
984 Werkneh, A., Rene, E., 2019. Applications of Nanotechnology and Biotechnology for Sustainable Water
985 and Wastewater Treatment, pp. 405-430.
986 Wu, F.-C., Tseng, R.-L., Huang, S.-C., Juang, R.-S., 2009. Characteristics of pseudo-second-order kinetic
987 model for liquid-phase adsorption: A mini-review. Chemical Engineering Journal 151(1–3), 1-9.
988 Yan, B., Isaure, M.-P., Mounicou, S., Castillo-Michel, H., De Nolf, W., Nguyen, C., Cornu, J.-Y., 2020.
989 Cadmium distribution in mature durum wheat grains using dissection, laser ablation-ICP-MS and
990 synchrotron techniques. Environmental Pollution 260, 113987.
991 Yuh-Shan, H., 2004. Citation review of Lagergren kinetic rate equation on adsorption reactions.
992 Scientometrics 59(1), 171-177.
993 Zeraatkar, A.K., Ahmadzadeh, H., Talebi, A.F., Moheimani, N.R., McHenry, M.P., 2016. Potential use of
994 algae for heavy metal bioremediation, a critical review. Journal of Environmental Management
995 181(Supplement C), 817-831.

996